THESIS

THE EFFECTS OF ION IMPLANTATION ON THE TRIBOLOGY OF

PERFLUOROPOLYETHER LUBRICATED, 440C STAINLESS STEEL COUPLES

Submitted by

Bradley A. Shogrin

Department of Mechanical Engineering

In partial fulfillment of the requirements

for the Degree of Master of Science

Colorado State University

Fort Collins, Colorado

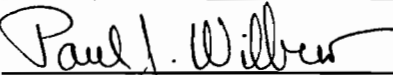December 1994

COLORADO STATE UNIVERSITY

August 25, 1994

WE HEREBY RECOMMEND THAT THE THESIS PREPARED UNDER OUR SUPERVISION BY BRADLEY A. SHOGRIN ENTITLED THE EFFECTS OF ION IMPLANTATION ON THE TRIBOLOGY OF PERFLUOROPOLYETHER LUBRICATED, 440C STAINLESS STEEL COUPLES BE ACCEPTED AS FULFILLING IN PART REQUIREMENTS FOR THE DEGREE OF MASTER OF SCIENCE.

Committee on Graduate Work

_____

_____

_____
Advisor

_____
Department Head

ii

ABSTRACT OF THESIS

ION IMPLANTATION EFFECTS ON THE LIFETIME OF PERFLUOROPOLYETHER LUBRICATED, 440C STAINLESS STEEL

The lubricating lifetimes of thin films of Krytox 16256N, a commercial perfluoropolyether used as a lubricant for space applications, in the presence of ion implanted 440C stainless steel was studied. Stainless steel discs, either unimplanted or implanted with Ti, Ti + N, Ti + C, N or C had a thin Krytox film (60-400 Å - verified using Fourier-transform infrared spectroscopy) applied to them reproducibly and uniformly ($\pm 15\%$) using a film deposition device developed for this study. Lubricating lifetimes of these films were determined by measuring the number of ball-on-disc, sliding-wear cycles required to induce an increase in the friction coefficient from an initial value characteristic of the lubricated wear couple to a final or failure value characteristic of an unlubricated, unimplanted couple. Test conditions included: dry nitrogen atmosphere, room temperature, 3 N load, and 0.05 m/s sliding speed. The lubricated lifetime of the 440C couple was increased by an order of magnitude by implanting with Ti. Implanting with Ti + C also yielded improvements, but implanting Ti + N, N and C did not. Ranked from most to least effective the implanted species were: Ti > Ti + C > unimplanted > N > C $\simeq$ Ti + N. The mechanism postulated to explain these results involves the formation of a passivating or reactive layer which inhibites or facilitates the production of Lewis acids that break down Krytox. The corresponding surface microstructures induced by ion implantation, obtained using X-ray diffraction and conversion electron Mössbauer spectroscopy, ranked from most to least effective in enhancing lubricant lifetime are: amorphous Fe-Cr-Ti > amorphous Fe-Cr-Ti-C + TiC > unimplanted > ε-$(Fe,Cr)_x N$, x = 2 or 3 > amorphous Fe-Cr-C $\simeq$ amorphous Fe-Cr-Ti-N.

ACKNOWLEDGMENTS

TABLE OF CONTENTS

LIST OF FIGURES

LIST OF TABLES

I. INTRODUCTION

Perfluoropolyethers (PFPEs) have been the liquid lubricants of choice for space applications for over twenty-five years because of their proven tribological performance and other attractive properties[1,2] such as low vapor pressure, low chemical reactivity, and the wide temperature range over which they remain a liquid. These fluorinated oils are used in such space mechanisms as actuators, antenna pointing mechanisms, filter wheels, gyroscopes, and scanning mirrors.[3,4] In the past few years there have been several incidents during which PFPE-lubricated space mechanisms showed anomalous behavior while in space.[5,6] These anomalies have been thought to be the result of PFPE degradation.

Over the past few years, a number of studies have focused on the degradation of the PFPE lubricants. Research has repeatedly shown that they degrade while in boundary-lubricated, sliding/rolling contact[7-19] and in elevated temperature-environments[20-27] by losing their desirable properties including lubricity. Such degradation could make component lifetimes limiting on longer missions, such as the space station mission with its 30-year operational lifetime. From the research that has been performed, few models have been proposed to explain the observed degradation. Research has suggested, however, that the rate of degradation is, in large part, dependent upon the surface chemistry between the substrate and the PFPE. The tests

1

showing this have involved heating or tribological testing of various substrates, that are representative of component surfaces, in the presence of PFPE lubricants.

Two possible solutions that have been proposed to increase lubricant lifetime are[1,14] 1) the use of soluble, boundary-lubricant additives and 2) chemical modification of the substrate surface. The addition of additives (antiwear, Extreme Pressure (EP), etc.) has been complicated by the fact that conventional additives used with hydrocarbon-based lubricants are not soluble in PFPEs.[2,14] The development of a new class of additives designed specifically for PFPE lubricants is under way.[28-30] Preliminary reports on their success in prolonging the lubricating lifetimes of PFPEs have been promising.[29,30]

The second proposed solution, which is addressed in this thesis, involves ion implantation to modify the substrate surface so that the degradation of the PFPE lubricant will be inhibited. This study is focussed on a space bearing steel (440C stainless steel). A demonstration of the effect of ion implantation on the PFPE-lubricated lifetime of the bearing material is sought rather than a detailed description of chemical decomposition mechanisms. The ultimate objective is to produce a more reliable, longer lasting, space-lubrication system.

Perfluoropolyethers, which were originally used as diffusion pump oils,[31] are extensively used as lubricants for magnetic recording media,[18] and are being considered for use in high temperature gas turbines.[32] There are presently four commercially available PFPEs, each of which comes in a variety of molecular weights. Their commercial names are Demnum, Fomblin Y, Fomblin Z and Krytox.

Of these four, Demnum and Fomblin Y have no space heritage.[1,2] The molecular structures of the four commercial PFPE lubricants are given in Table 1.

Table 1. The Molecular Structure of Four Commercial PFPEs (From Ref. 20, Fig. 1)

PFPE	Molecular Structure
Demnum	$CF_3-CF_2-CF_2-O-\left(-CF_2-CF_2-CF_2-O-\right)_m-CF_2-CF_3$
Fomblin Y	$CF_3-O-\left[-\underset{\underset{CF_3}{\mid}}{CF}-CF_2-O-\right]_m-\left(-CF_2-O-\right)_n-\left[-\underset{\underset{CF_3}{\mid}}{CF}-O-\right]_o-CF_3$ $m/n/o = 40/1/1$
Fomblin Z	$CF_3-O-\left(-CF_2-CF_2-O-\right)_m\left(-CF_2-O-\right)_n-CF_3$ $m/n=2/3$
Krytox	$CF_3-CF_2-CF_2-O-\left[-\underset{\underset{CF_3}{\mid}}{CF}-CF_2-O-\right]_m-CF_2-CF_3$

Demnum and Fomblin Z are linear molecules whereas Fomblin Y and Krytox are designated as branched, because they contain the pendant side groups, CF_3. As the

numbers of monomer units (m, n, or o), each ~6 to 8 Å in diameter,[7] increase, the polymer becomes longer and its molecular weight increases. All are considered to have low chemical reactivity, but their other properties are determined by their molecular weights and structures. For example, higher molecular weights yield lower vapor pressures and higher viscosities. For this study, the high molecular weight lubricant Krytox 16256 was used. This PFPE has an average molecular weight of 11000 amu, a vapor pressure of 3×10^{-14} Torr and a viscosity of 2717 mm^2/s, both at 20 °C.[33]

Even though PFPEs have a low chemical reactivity, they can react and the reactions can facilitate their degradation. Reaction temperatures can be increased to accelerate this process so the mechanism by which PFPEs lose their lubricating properties may be studied more conveniently. These so-called thermal-degradation studies, in which controlled heating of a fluid in the presence of a selected substrate takes place, are designed to: 1) determine the temperature at which a fluid begins to decompose, and 2) determine reaction products and thereby infer the chemical reactions associated with fluid decomposition. Carré[24] performed PFPE thermal-degradation experiments using Krytox mixed with the Lewis acids AlF_3, $AlCl_3$ and FeF_3 in powdered form under a N_2 atmosphere. These three Lewis acids, which are inorganic compounds prone to accept an electron pair, all caused the decomposition temperatures to decrease relative to the case where no Lewis acid was present. Specifically, the Krytox decomposed at 200 °C in the presence of $AlCl_3$ and at 350 °C in the presence of AlF_3 and FeF_3 compared to 375 °C when no Lewis acid

4

was present.

Kasai,[20,21] going a step further, has shown that the thermal catalytic degradation of a PFPE is dependent upon the strength of the Lewis acid and has proposed a chemical degradation mechanism for each of the four commercial PFPEs. He postulated a mechanism in which the Lewis acid acts as a catalyst that promotes an intramolecular disproportionation reaction that results in chain degradation. Although the details of the chemical reactions observed by Kasai go beyond the scope of this report, it is interesting to note that the reaction took place either within the PFPE chain (resulting in two fragmented chains) or on the chain ends (resulting in a shortened chain and a lower molecular-weight product). The location of the reaction depended on the particular PFPE. Specifically, he found Fomblin Y and Z were attacked at their internal acetal units, $O-CF_2-O$, and that chain fragmentation resulted. Demnum was also attacked at internal sectors, whereas Krytox was attacked at chain ends. He also found that these fragmented or shortened chains are susceptible to further breakdown, again catalyzed by Lewis acids, that eventually result in complete degradation of the PFPE. Kasai's results show the importance of the presence and relative strengths of Lewis acids in promoting PFPE degradation.

Other thermal degradation studies designed to look at the effects of certain metals or metal alloys in the presence of particular PFPEs have shown that PFPE degradation is highly dependent upon the type of substrate. For example, PFPE lubricants have been shown to degrade at lower temperatures in the presence of M-50 steel and Ti-4Al-4Mn than they do when they are in contact with pure titanium or

5

pure aluminum.[25-27] Hence, it appears that the surface chemistry of the specimen being tested affects the rate of PFPE degradation.

PFPEs have also been observed to break down chemically while in boundary lubricated contact with steels.[7,9,10,14-16] In all of these cases the formation of the Lewis-acid catalyst FeF_3 was observed on the wear track after the initiation of sliding. Unlike the thermal degradation tests, tribological tests involve an extremely small amount of fluid (μg) in the contact with much smaller surface areas. Because of this, the rate of generation of chemical products is low and it is difficult to detect them over a reasonable time period. This has made it difficult to identify a complete and detailed mechanism of chemical breakdown. Although the mechanism of chemical breakdown is not well understood, there are hypotheses. The most widely referenced hypothesis is that of Carré[9] who proposed that the Lewis acid is formed after the native oxide of the steel has been rubbed off and fresh, highly-reactive metal is exposed to the fluorinated oil. As sliding/rolling persists, the Lewis acid continues to form and break down the PFPE catalytically.

Mori and Morales[16] confirmed the catalytic process when they observed that contact between a 440C ball and disc caused FeF_3 to form and induce the formation of degradation products. However, a recent study by Herrera-Fierro, Jones and Pepper[7] shows no measurable reaction takes place between an oxide-free 440C surface and Fomblin Z in vacuum at room temperature under static conditions. Reactions between the oxide-free surface and PFPE did occur in the Herrera-Fierro experiment at elevated temperatures (190 °C). They were also observed when the oxide-free

material was rubbed with a 440C ball, that yielded asperity temperatures estimated to be < 100 °C. In those two situations, similar decomposition by-products, including FeF_3, were observed. A similar study with Fomblin-Z-lubricated sapphire (Al_2O_3) performed by the same group[8] resulted in the decomposition of the PFPE when sliding was initiated. In this case, it was observed that the Lewis acid AlF_3 had formed in the contact area. In the same study it was shown that Fomblin Z reacted with oxide-free aluminum at room temperature, even when there was no tribo-contact, and that similar by-products, including AlF_3, were observed.

It has been proven in thermo-chemical studies and inferred in tribo-chemical experiments that Lewis acids promote PFPE degradation. Therefore, one way to inhibit tribo-induced degradation may be to utilize a surface that does not promote the formation of Lewis acids in the presence of fluorinated oils. Carré[13] demonstrated that the PFPE-boundary-lubricated wear life was increased by a factor of 5 to 10 by using TiN coated 440C test specimens. TiC coated 440C and Si_3N_4 ceramic ball bearings have also been shown to have greater tribological longevity compared to their 440C counterpart when all were PFPE lubricated.[11,13,14] In Carré's studies[13,14] it was concluded that the hard coatings and ceramic material prevented the formation of Lewis acids, thus halting the Lewis-acid-induced degradation of the PFPE. The thesis of this work is that a 440C stainless steel surface can be implanted with ions that will passivate it, thereby retarding the formation of the iron fluoride and enhancing the lubricant lifetime.

Ion implantation is a surface-treatment technique that can be used to modify

the surface properties of materials without affecting either the properties or dimensions of the bulk material beneath the treated layer. By introducing a foreign specie into a sub-micron surface layer, ion implantation can induce unique surface microstructures. In the present case it enables a designer to retain 440C as the material in a bearing and simply modify its surface. As a result, the broad space experience obtained with 440C steel bearings could continue to be utilized and it would not be necessary to seek a new material that would be more compatible with PFPE lubricants.

Ion implantation is widely used to dope semiconductors but it is rarely used to alter friction and wear properties. In 1973, however, Hartley et al.[34] conducted experiments on the tribological effects of high-energy (500 keV) Mo, Sn, Pb, In, Ag, S, and Kr ions implanted into steel. They found that while Kr implanted into a steel induced no noticeable change in its friction behavior, the friction coefficients could be increased or decreased up to 50% relative to the unimplanted steel by implanting other species. It was concluded that surface microstructures could be tailored to produce more appealing tribological surfaces by implanting selected species into the sub-micron surface layer of a virgin material. Since then extensive research in the area has shown that ion implantation can improve the properties of materials related to their wear,[35-44] friction,[43-46] corrosion,[47,48] and fatigue[46] characteristics. The main focus of these works has been on steels because they are widely used in tribological applications and there is the possibility of saving many billions of dollars annually if their tribological, corrosional and/or fatigue properties can be improved.

8

An example of the effectiveness that ion implantation can have on steel is found in the work by Wei et al.[35] which showed that implantation of 304 stainless steel discs with nitrogen could induce a two-to-three-order-of-magnitude increase in its resistance to galling. In another example, Singer et al.[45] demonstrated that titanium implanted into 52100 steel induced a decrease in friction coefficient from ~ 0.6 to ~ 0.3.

The ion-implantation process utilizes atoms that are ionized and then accelerated in an electric field to a high kinetic energy before they are directed into a substrate. These ions travel through the atomic layers of the substrate, colliding with, displacing and reflecting off of the atoms. Collisions between the incoming high-energy ions and atoms causes displacements that create atomic-level voids or vacancies. Eventually, the ion comes to rest and either sits interstitially or substitially among neighboring atoms. The culmination of the addition of foreign ions and the defects produced can give rise to new microstructures in the substrate and this can be controlled by implanting the proper specie under the proper processing conditions.

In this study the effect of implantation conditions on the lifetime of a PFPE-lubricated 440C couples in sliding contact was studied. It should be noted that the results obtained here are preliminary. Carbon, nitrogen and titanium ions were investigated because these implanted species have shown to induce tribological improvements.[34-46,48,49] The main objective of this work was to determine the effect of five implantation conditions on the lifetime of a Krytox-boundary lubricated, 440C-stainless-steel couple.

II. APPARATUS AND PROCEDURES

A. Summary of Experimental Approach

A number of 440C steel discs, some unimplanted, others implanted at one of five alternative conditions, each with an accompanying 440C steel ball, were used in this study. The microstructures induced by ion implantation of these discs were characterized using both backscattered conversion electron Mössbauer spectroscopy (CEMS) and x-ray diffraction (XRD). A number of the discs, both implanted and unimplanted, were coated with Krytox 16256N using a unique method which yielded a thin, reproducible, uniform film. The thicknesses of the applied PFPE films were determined using Fourier transform infrared spectroscopy (FTIR). A fixed-ball-on-disc tribometer was utilized to measure the tribological characteristics of both the lubricated and unlubricated disc/ball pairs. In an effort to maximize their usefulness, each disc had multiple wear tracks worn on its surface. The friction coefficient was recorded for each wear track and was used as the indicator of lubricant/implanted-layer failure.

B. Materials

Fully hardened 440C stainless steel (BHN = 500) suitable for space bearing applications was used in this study. Discs and balls made from the material were slid

against each other to produce a circumferential wear track on the disc and a worn spot on the ball. Hardened 440C is a martensitic steel that is processed by sequentially raising its temperature into the range between 845 and 900 °C, quenching, and finally tempering at 315 °C. The 440C stainless steel alloy is composed of 16-18 wt% Cr, 0.95-1.2 wt% C, 1.0 wt% Si, 1.0 wt% Mn, 0.04 wt% P, 0.03 wt% S and the remainder Fe.

The 440C discs were 17.46 mm (11/16") in diameter and 4.76 mm (3/16") thick. The grade 10, 440C balls used in the study were 9.53 ± 0.00102 mm in diameter ($3/8" \pm 0.00004"$). Each disc and ball had a mirror finish (arithmetic roughness average, $R_a \approx 0.01$ μm). A total of twenty-nine discs, lubricated and unlubricated, each with an accompanying unlubricated ball were used in this study. Eighteen of these discs were cleaned, implanted and then subjected to a sliding wear test. The remaining eleven (designated unimplanted) were cleaned as received (unimplanted) and then subjected to the same sliding wear test. None of the bearing balls were implanted.

C. Ion Implantation and Sample Designations

All to-be-implanted discs were first cleaned in an ultrasonic cleaner for approximately 10 minutes each in a sequence of three different solvents. Trichloroethane (NU) was used first to remove any heavy oils that might be present. This was followed by acetone to remove NU residues and then finally by methanol to remove water vapor contaminants. After cleaning, the discs were implanted using ion

implanters designed to produce either metal or gaseous ions. The metal-ion implanter[50] differs from the gaseous-ion implanter[51,52] in that its source is designed to induce vaporization of the metal placed in it by electron-bombardment heating. This difference aside, the implanters perform similarly. In the ion source of each, high energy electrons bombard the vaporized atoms or gaseous atoms and ionize them and produce a plasma. Ions are extracted from the plasma through holes in a pair of plates between which an electric field has been applied. Both implanters utilize ion-propulsion technology and are designed to produce broad ion beams that operate at high-ion-beam current densities (i.e. high dose rates) and facilitate rapid treatment of substrates. The dose rate and energy capabilities for the metal-ion-implanter, range from 100 to 700 μA/cm^2 and 10 to 50 keV, respectively. Whereas, for the gaseous implanter, values range from 10 to 1500 μA/cm^2 and 10 to 80 keV, respectively. The temperature of the substrate, while being implanted, can be controlled quite precisely. This is accomplished by 1) clamping the substrate to a water-cooled, copper heat-sink, 2) placing a material with the proper thermal conductance between the heat sink and sample and 3) adjusting the current density and/or energy of high-energy ions impinging on the substrate surface. The temperature of the substrate is constantly monitored during implantation using an iron-constantan thermocouple. More complete descriptions of the implanters are given in the literature.[50-52]

Five implantation conditions were chosen for the study on the basis of improved wear and friction properties observed in previous tests. The five implantation conditions, the designations of discs implanted at each condition, as well as the

designations of discs tested in the unimplanted state are given in Table 2.

Table 2.   Description of the 440C Discs Used in the Study

Disc Numbers	Implanted Specie	Backfill	Energy (keV)	Dose Rate (μA/cm^2)	Dose (ions/cm^2)
125,165,167, 179	Ti	None	50	200	2.0×10^{17}
153,**157**,171	Ti	N_2	50	200	2.0×10^{17}
149,174,175, 177	Ti	CH_4	50	200	2.0×10^{17}
141,169,**172**, 183	N_2	None	60	100	1.0×10^{17}
161,173,181	CH_4	None	60	100	2.0×10^{17}
204,238,191, 201,216,196, 208,240,188, 189,244	Unimplanted	—	—	—	—

Bold numbers designate discs tribo-tested under unlubricated conditions.

Three of the five implantation conditions involved titanium implantation either alone or with a backfill gas (nitrogen or methane). In the latter cases, the backfill-gas partial pressure was maintained at 2×10^{-5} Torr to ensure a backfill-molecule arrival rate that was an order of magnitude greater than the ion arrival rate. This relative balance is considered adequate to assure substantial entrainment of the backfill gas into the layer along with the Ti which is a strong getter of both N and C. The remaining two implantation conditions identified in Table 2 involved implantation of

13

carbon (as CH_4) or nitrogen.

Since wear testing of the implanted layers was conducted for short durations under sliding, low-Hertzian-pressure, boundary-lubricated conditions, it is argued that the active tribological region on the disc was very thin (< 0.1 μm). Ion-implanted layers with thicknesses of this order can be produced using modest implantation energies and low surface temperatures. The energies indicated in Table 3 (50 or 60 keV) are sufficient to assure ion ranges in the 440C substrate that are of the order of 0.1 μm. Consequently, implanted-ion diffusion was not required to enhance the layer thickness and the substrates could be maintained at a low temperature (< 100 °C) during processing. This temperature is sufficiently low so it can be assured that no softening of the bulk material occurs during implantation. The maximum benefit of a specie implanted at a given energy and a low temperature is expected at the saturation dose where the concentration profile in the layer becomes invariant with dose. For the energies and substrate temperatures used in this study the saturation dose as reported in the literature,[53,54] which is 2 x 10^{17} ions/cm^2, was used.

D. Microstructural Characterization

Because research has shown that the rate of PFPE degradation in boundary-lubricated contacts with 440C steel is, in large part, dependent upon the surface chemistry between the substrate and the PFPE, it was considered important to determine changes induced in the 440C by implanting it. Each of the five

implantation conditions was expected to induce different microstructures and compositions, and, therefore, different surface/lubricant chemistries. Because wear under boundary lubricated conditions involves contact between asperities on the ball and disc surfaces and this can result in removal of these asperities, it is desirable to measure the microstructures and compositions to depths that extend significantly beyond typical asperity dimensions (~ 0.01 μm).

Implantation-induced microstructural and compositional changes were determined using backscattering conversion electron Mössbauer spectroscopy (CEMS)[68,69] and x-ray diffraction (XRD) because they yield information over the required depth. In addition, both techniques are nondestructive so they can be used to make measurements on the actual discs that will be subjected to tribo-testing. The CEMS technique senses iron nearest-neighbor information in a surface layer with a thickness that is about equal to the implantation depth (~ 0.1 μm). This information can, in turn, be used to determine the bonding of Fe atoms to each other and to other atoms and the relative concentration of these bonds. The bonding in turn determines the phases and microstructures that are present.

The CEMS technique uses a radioactive source, in this case ^{57}Co, to direct 14.4 keV γ-rays onto the surface of interest. These γ-ray photons typically interact with ^{57}Fe atom orbital electrons in the sample and through a resonance mechanism called the internal conversion process, produce energetic electrons that are detected in the Mössbauer equipment. Because the γ-ray source is oscillated in a low-frequency, small-amplitude motion, the photons coming from it experience a very modest

doppler-induced dispersion about their 14.4 keV mean energy. Nearest neighbor bonding to the ^{57}Fe atoms changes the resonant energy of their orbital electrons and causes photons with doppler-shifted energies to induce internal conversion electrons. The Mössbauer spectroscopic signature is produced by correlating the production of these electrons with γ-ray source velocity which is in turn proportional to the doppler shift. The depth, over which bonding information is sensed (~ 0.1 μm), is determined by the fact that this is the mean free path for absorption of internal-conversion electrons in steel.

X-ray diffraction measurements were also made to provide verification of CEMS results. They were made using equipment based on the symmetric Bragg-Brentano geometry in which the angles of incidence and reflection are maintained equal. The x-rays with a wave length of 1.5406 μm were generated using a Cu K$_{\alpha}$ source. The XRD probe depth is approximately 2 μm.

E. Preparation for Wear Testing

Special care was exercised to ensure meticulous, reproducible surface cleanliness for each disc-and-ball couple prior to lubricant application on the disc or tribo-testing if no lubricant was applied. This was necessary because contaminants left on the surfaces could influence the chemical boundary layer between it and the lubricating PFPE. In addition, organic contaminants on surfaces in sliding contact have been known to form friction polymers (organic lubricating films).[55] Such polymers could affect both friction coefficients and the PFPE oil decomposition rates,

because the metal would not be in direct contact with the PFPE at the sliding contact.

The cleaning was accomplished by placing a disc/ball pair in an ultrasonic cleaner, first in hexane to remove any heavy oils, then in acetone and finally in methanol; each for approximately 10 minutes. After methanol cleaning, samples were blown with dry nitrogen to evaporate both the methanol and any water residue that might have been left on the sample surface after the hydrous methanol had evaporated. The couple was then immediately covered to minimize dust contamination. Finally, samples were exposed to an ultraviolet/ozone (UV/ozone)[56-58] environment for 15 minutes to remove carbonaceous contamination which develops during exposure to the atmosphere. This layer reforms within 10 to 15 minutes after UV/ozone treatment if the surface is left exposed.[59] Discs and balls that did not have PFPE applied to them were put into a dry N_2 atmosphere within 5 minutes after the completion of UV/ozone treatment and were kept there until ready for tribo-testing. Discs that had PFPE applied to them were coated within 5 minutes of UV/ozone treatment and then placed in the same dry N_2 environment and held at or below 25 °C to inhibit the PFPE/substrate reaction.

Application of a uniform, reproducible coating of PFPE with a controlled thickness is a difficult task. For this reason, the majority of the tribological tests performed in the past using PFPE lubricants have been conducted under flooded lubricant conditions. However, flooded testing is undesirable when the object of the test is to determine the lifetime of a lubricant that decomposes in the presence of two surfaces in sliding contact. A precisely controlled, relatively small amount of

17

lubricant, on the other hand, should yield reproducible lifetime results in reasonable test times. In order to obtain meaningful results that would satisfy the objectives of this study, it was determined that the PFPE film should be uniform, controllable and thin (a few hundred angstroms).

Several methods of applying the PFPE were investigated and a derivative of the process known as "dipping" was found to yield the desired reproducible, uniform, controlled thickness. Dipping is the process of coating a specimen by slowly withdrawing it at a constant speed from a diluted mixture of the fluid to be coated (solute) in a highly volatile solvent. As the sample slowly leaves the mixture, its surface is covered by a film of the solution. Soon thereafter the solvent evaporates leaving a thin solute layer on the surface. In the dipping procedure both the concentration of the mixture and withdrawal speed have been shown to be important parameters that influence the resulting thickness.[60] Either a higher concentration of solute or a greater withdrawal speed results in a thicker coating.[60] Unfortunately, commercial dipping apparatuses are expensive, mainly because of the costly control system needed for constant-speed withdrawal of the sample. To avoid these high costs, an effective and inexpensive derivative of dipping was developed. The associated apparatus, seen in Figure 1, is referred to as the Film-Deposition Device (FDD). In this device, gravity causes constant-velocity motion of the fluid past a stationary disc and this produces a high quality thin-film without the expensive control system. In order to apply a coating for this study, a disc was positioned in the solution as shown in Figure 1. The stopcock of the FDD was opened and the mixture

18

Lubricant/
Solvent
Solution—

— Specimen

CD-94-64838
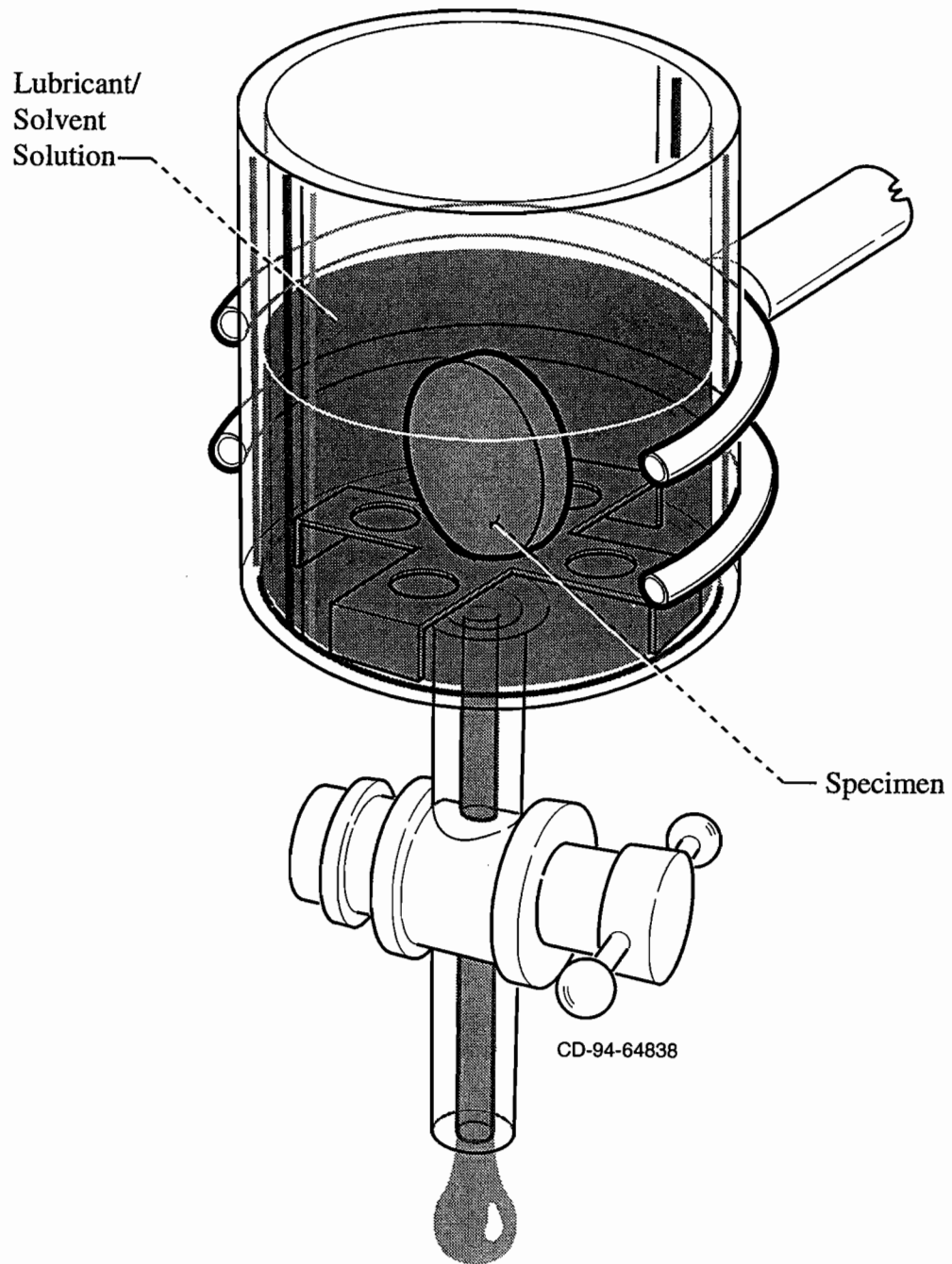
Figure 1. Film Deposition Device (FDD)

19

was allowed to flow out the bottom through a 1.0-mm-bore hole. The speed at which the liquid level dropped past the upright sample, that is, the withdrawal speed, was measured and found to be 0.8 mm/sec.

The mixtures applied to the discs using the FDD contained different concentrations of Krytox 16256N (lot number 60164-51-4) in Vertrel 245 [1,1,2,2,3,4-hexafluoro-3,4-bis(trifluoromethyl) cyclobutane]. Vertrel 245, and the substance it is helping to replace (Freon-113) are two of a very limited number of solvents that are effective in dissolving Krytox. The unimplanted discs not identified by bold numbers in Table 2 were coated using a LDD mixture having concentrations of 1.0, 3.0 or 5.0 grams of Krytox 16256N in 100 ml of Vertrel 245. These discs were then tribo-tested to determine the effect of lubricant thickness on lubricant lifetime in the 440C ball/440C untreated disc sliding wear environment. On the basis of these tests, it was determined that the thinnest lubricant layer investigated was preferred because it could be applied reliably and it yielded consistent wear test results in a reasonable period of time. Hence, these thinnest layers of Krytox 16256N (1.0 gm in 100 ml of Vertrel 245) were applied to the implanted discs (those not shown bold in Table 2).

F. Krytox Film Thickness Measurements

Thicknesses of Krytox 16256N films applied to each disc were measured using a Nicolet 740 Fourier-transform infrared (FTIR) spectrometer[61,62] that utilizes a grazing angle objective and is operated in the reflectance mode. The measurements

were made using an angle between the incident, 100 μm diameter photon beam and the normal to the surface of $\sim 75°$ (i.e. a grazing angle $\sim 15°$). In the reflectance mode, beams of photons, each characterized by a narrow band of IR wavenumbers within the overall range from 700 to 4000 cm^{-1}, are directed onto a substrate. These photons travel through the lubricant film, reflect off of the metal surface behind it and pass back through the film and on to a detector. While passing through the film, photons with a wavelength corresponding to the vibrational frequency of the molecules present are absorbed by these molecules. Because photon absorption in the film is a function of photon wavenumber, this procedure yields an absorbance vs. wavenumber signature that characterizes the film. Absorbance at a particular wavenumber is defined by the expression

$$A = -\log I/I_o$$

where

I = intensity of the beam at the wavenumber that has passed through the film,

I_o = intensity of the beam at the wavenumber that reflects off of an uncoated substrate (i.e the background signal).

The above relationship between absorbance and intensity ratio is based on the Beer-Lambert-Bouguer law. This law and additional physical details of the absorption process are given elsewhere.[61-63]

In order to obtain a high signal to noise ratio to assure accurate Krytox-thickness measurements, the wavenumber scanning process was repeated 400 times.

21

To verify film uniformity across each disc, these absorbance vs. wavenumber spectra were taken in three locations near the outer edge of each disc, $\sim 120°$ apart. The absorbance vs. wavenumber signature shown in Figure 2 is typical of those observed for a Krytox film. It shows that Krytox absorbs photons having wavenumbers near 1313, 1280, 1190, 1170, and 980 cm^{-1}. The particular absorbance vs. wavenumber plot of Figure 2 was generated from a 440C disc that had a 430 Å thick Krytox film deposited on its surface.

Because the absorbance signal at 1313 cm^{-1} is large, this signal is the one that has been correlated with film thickness. This correlation, which has been accomplished and reported by Pepper,[64] is reproduced as Fig. 3. Pepper verified the Krytox data in this figure by measuring film thicknesses using ellipsometry (over a wide range of incident beam angles and wavelengths) and then making FTIR absorbance measurements on the same films.

G. Tribological Testing

Tribological testing of each disc was performed either after the PFPE thickness had been measured (lubricated discs), or after UV/ozone treatment (unlubricated discs). It was performed on the fixed-ball-on-disc tribometer shown in Figure 4. The angular velocity of the disc was maintained via the drive motor to obtain a relative sliding velocity between the disc and ball of 0.05 m/s. A 3-N normal load between the ball and disc was applied via the lever arm and gimbal and it induced an initial Hertzian contact pressure[65] of ~ 0.69 GPa at the disc surface. This pressure, which

22
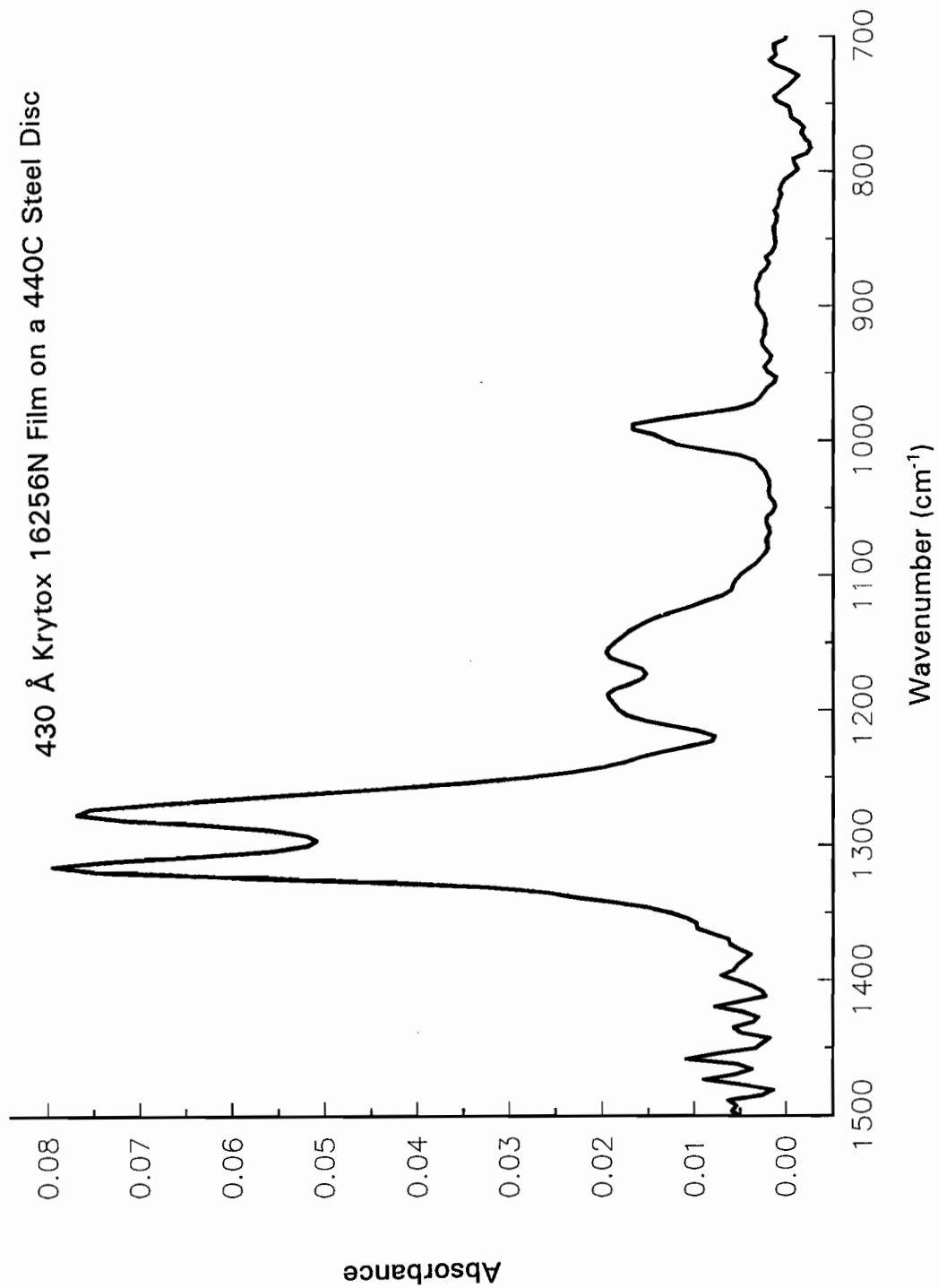
Figure 2. Typical FTIR Spectra for a 430 Å Film on a 440C Steel Disc
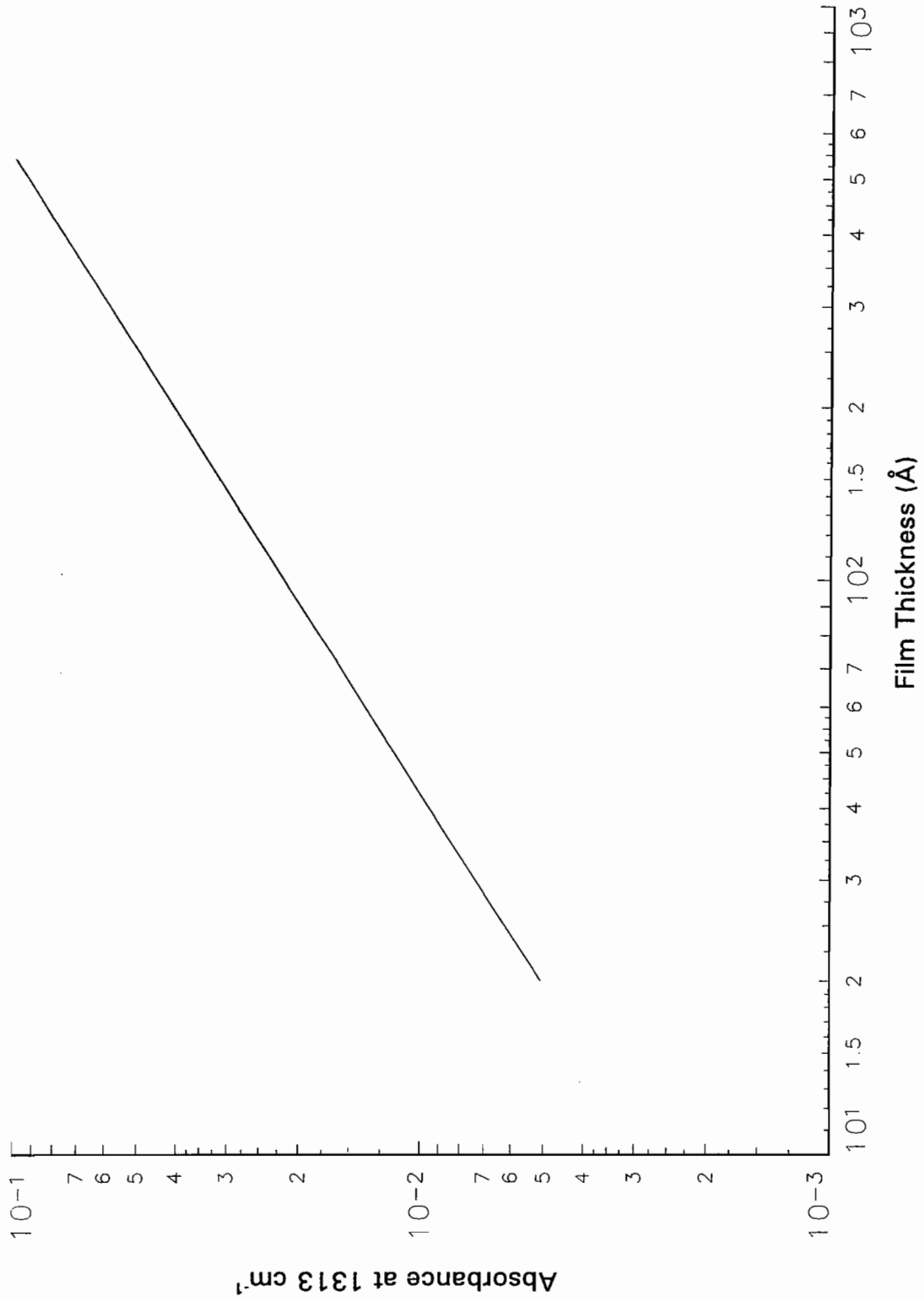
Figure 3. Theoretical Correlation of Spectral Absorbance and Krytox Film Thickness

Ball

Wear Track

Disc

DETAIL

Drive Motor

Digital Counter

Gimbal

Sensor Preload

Load

Friction Force Sensor
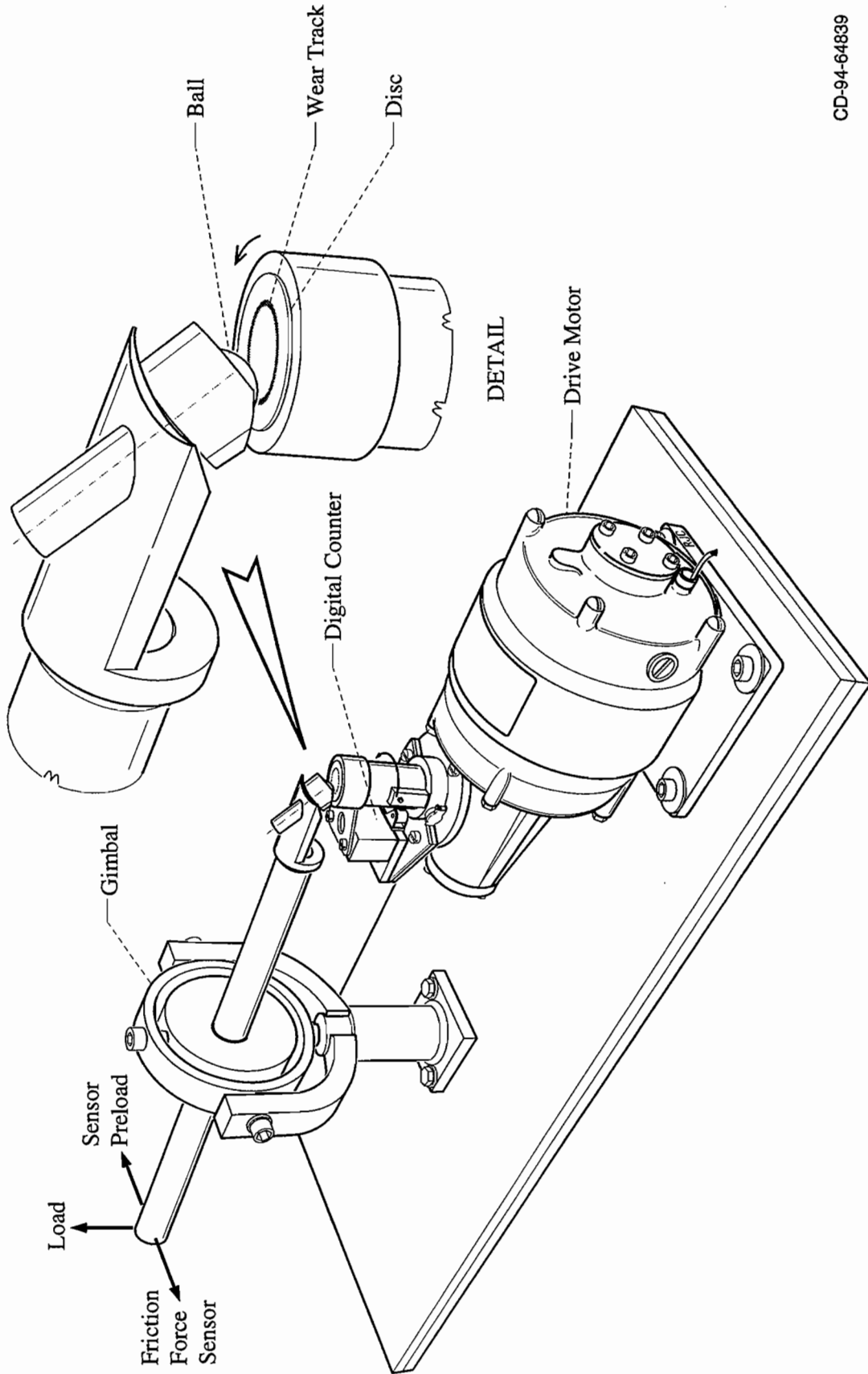
CD-94-64839

Figure 4. Ball-on-Disc Tribometer

is roughly 35% of the yield strength of 440C steel, decreased as ball wear occurred and the contact area between the ball and disc increased. The friction force was obtained by amplifying the resulting signal from a wheatstone-bridge strain gage sensor. Along with the friction force, the number of disc revolutions were counted electronically during each test.

After a test, the ball support fixture and ball were rotated to expose an unworn surface on the ball and the fixture was extended so the ball would contact the disc at a different radius. By doing this, three wear tracks, 1.59 mm (1/16") apart, could be and generally were worn on the surface of each disc.

The ball-on-disc apparatus was enclosed in a plexiglass box to minimize dust contamination and to facilitate environmental control. Tests were run in dry N_2 to minimize surface film formation (i.e. oxides, friction polymers, etc.). Tribological testing in dry N_2 has been shown to simulate a vacuum environment adequately.[6,63,66] Ambient temperatures were not controlled during the tests but were estimated to be ~ 25 °C.

III. RESULTS

A. Summary

The basic thesis of this work was that failure of a PFPE lubricant film applied to a disc would be accompanied by an increase in the friction coefficient to a level typical of unlubricated discs. The mean friction coefficient of unlubricated, unimplanted discs was, therefore, measured to define a failure threshold. The number of disc rotational cycles required to exceed this threshold was then established as the measure of performance. Using this performance measure, friction measurements were made on several wear tracks on unimplanted discs coated with various thicknesses of Krytox. The tests showed the thinnest lubricant films gave the most reproducible results and required the shortest test times. Krytox films of this thickness were then applied to the implanted discs and cycle histories of their friction coefficients were measured. The influence of the ion implantation was then determined by comparing cycles to failure for the various processing conditions with cycles to failure for the unimplanted discs. Reasons for the differences were sought via results obtained from analysis of the implanted surfaces.

B. Establishment of the Lubricant-Failure Criterion

Lubricant failure was said to occur in these tests when the friction coefficient

measured using the fixed-ball-on-disc tribometer rose from an initial relatively low value to a value typical of an unlubricated, unimplanted disc. When this occurred it is argued that the protective layer(s) (applied lubricant and/or implanted layer) either wore off, ruptured or broke down, thereby allowing fresh 440C metal of the disc to come into contact with the fresh 440C metal on the ball. Figure 5 shows the mean friction coefficient vs. cycle number of three wear tracks on two separate discs that were tested unlubricated and unimplanted. Mean friction coefficient as used in this thesis is the mean of the friction coefficients of the complete revolution over the indicated cycle. Typically, friction-coefficient fluctuations over a cycle were ± 0.05 about the mean for these data. The mean friction coefficient data in Fig. 5 all lie between 0.8 and 0.63. Thus, it is argued that an increase in mean friction coefficient above 0.63 is indicative of failure and 0.63 is defined as the failure limit for a lubricant film (i.e. values above this are indicative of metal-on-metal contact). The numbers of rotational cycles that can be applied to the lubricant film on a wear track before the friction rises above the failure limit is, therefore, the film lifetime.

Since surfaces were modified using ion implantation before films were applied in the proposed tests, it was also important to know if implantation processing itself changed the failure limit, i.e. if a 440C ball contacting an unlubricated, implanted 440C disc yielded the same lower limit on friction coefficient. Figure 6 shows typical friction-coefficient histories for discs implanted with the various ions that were used in these tests. They indicate that the implanted surfaces do exhibit lower mean friction coefficients (~ 0.3) at the start of testing, but they rise above the failure line

28
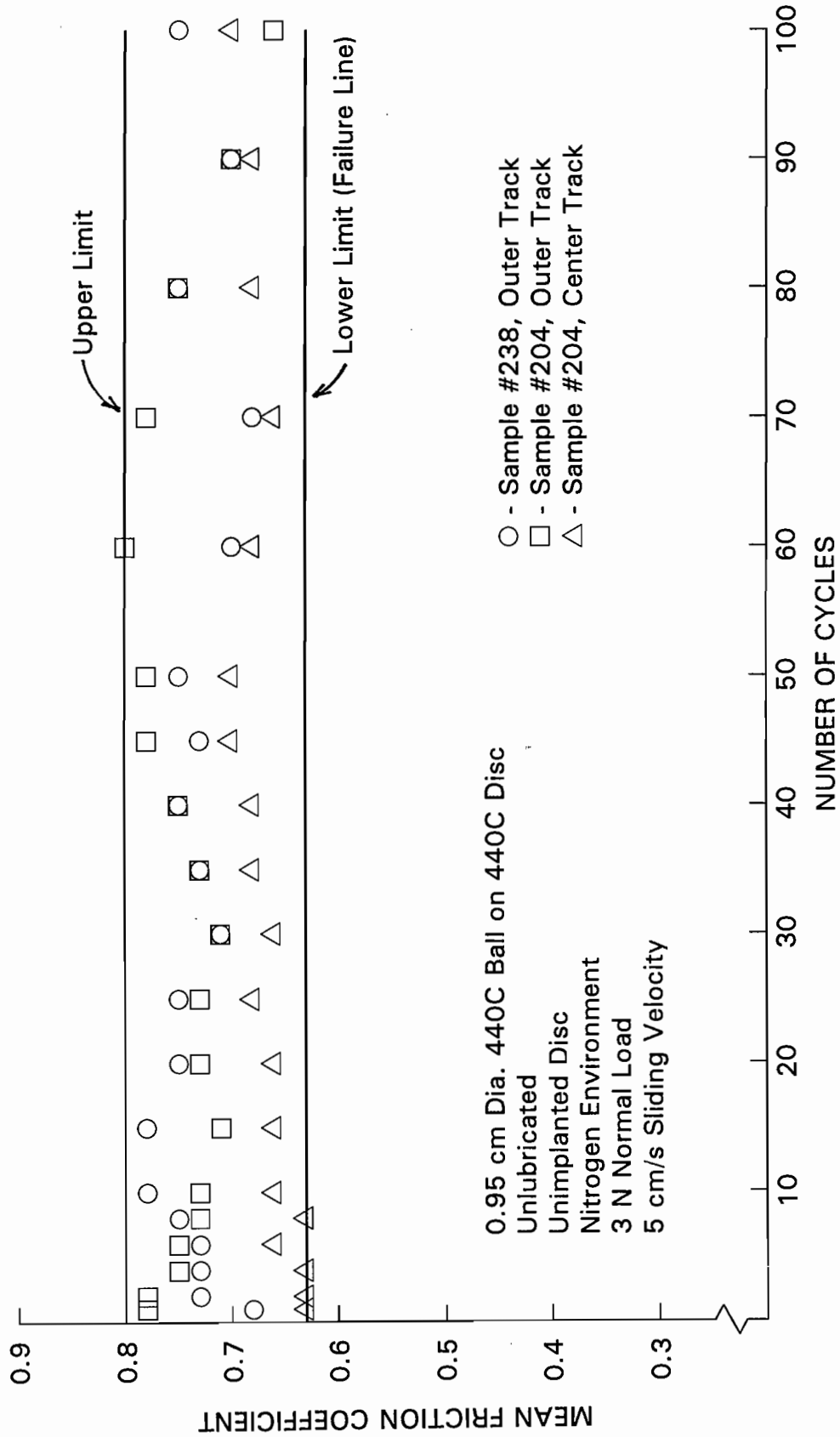
Figure 5. Typical Friction Coefficient Data for Unimplanted, Unlubricated Discs
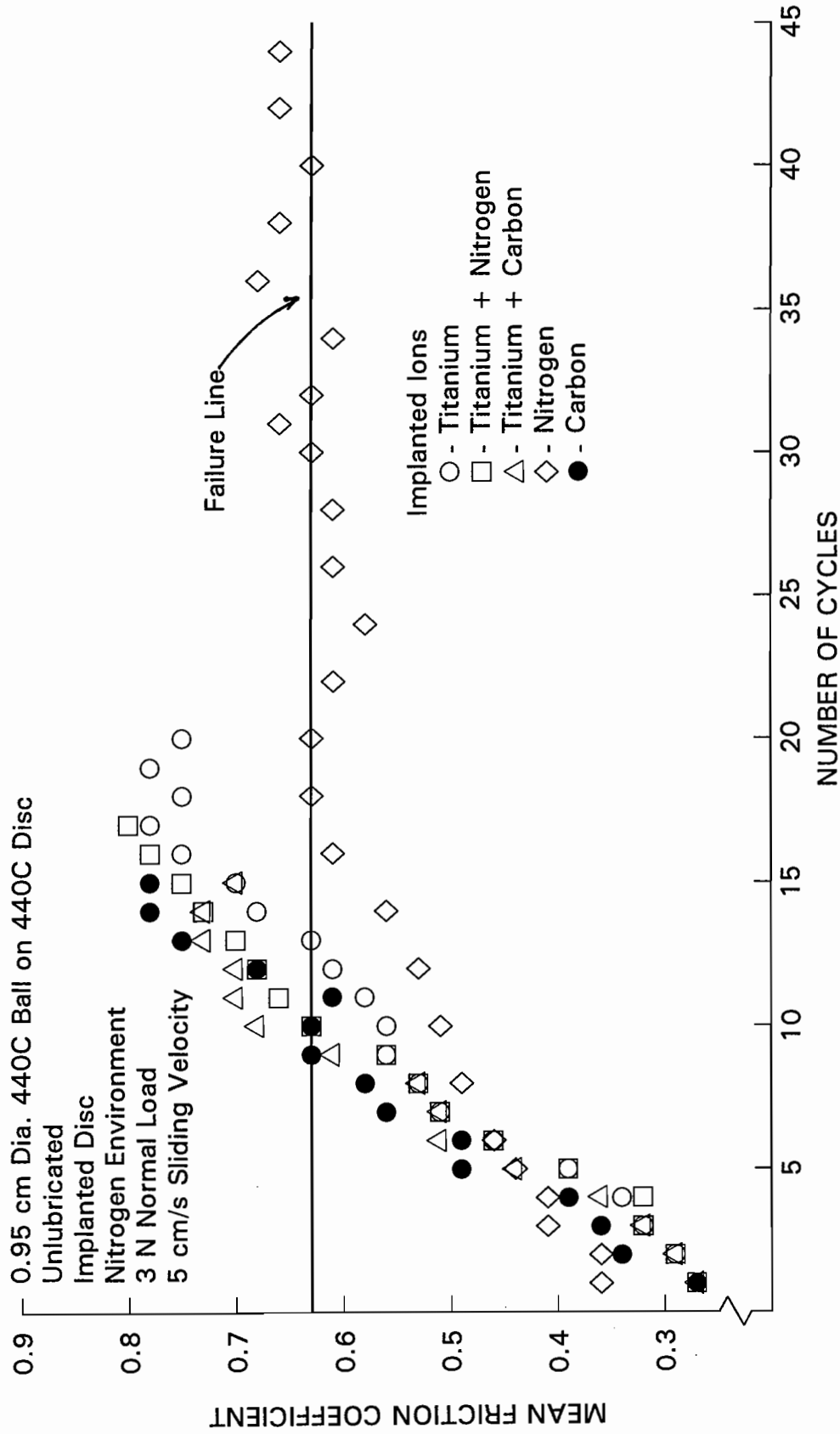
Figure 6. Typical Friction Coefficient Data for Unlubricated, Ion-Implanted Discs

within about 10 to 15 cycles for all but the N-implanted surfaces which requires ~18 cycles. Table 3 contains data obtained in a large number of tests conducted at each implantation condition. These results are consistent with the typical results in Fig. 6. The average values appear outside the parentheses, whereas the observed ranges are contained within the parentheses. All of these data suggest that the uncertainty in lifetime is extended by no more than about 30 cycles as a result of the implantation itself.

Table 3. Unlubricated Wear Test Results

Surface Treatment (Disc Designation)	Initial Mean Friction Coefficient	No. of Cycles Until Failure	Tracks Tested
Titanium Implanted-No Backfill (125)	0.32 (0.27-0.36)	12 (11-13)	4
Titanium Implanted-N_2 Backfill (157)	0.29 (0.27-0.32)	8 (7-10)	3
Titanium Implanted-CH_4 Backfill (149)	0.28 (0.27-0.29)	11 (10-12)	2
N_2 Implanted (172)	0.34 (0.32-0.36)	30 (11-58)	4
C Implanted (161)	0.27 (0.24-0.29)	8 (7-9)	4

C. Lubricant Thickness Results

In order to select a lubricant thickness that would yield reasonable test-times-to-failure, unimplanted discs were coated with Krytox 16256N films having different thicknesses and they were then subjected to tribological testing. Thicknesses of the

Krytox 16256N films were determined by making FTIR measurements of the absorbance at the 1313 cm^{-1} wave number and then using Fig. 3. The FTIR absorbances measured at three locations on each unimplanted-lubricated disc, along with the corresponding average Krytox 16256N thickness obtained from Fig. 3 are shown in Table 4.

Table 4. FTIR Absorbance and Extrapolated Average Krytox Thicknesses for Unimplanted-Lubricated 440C Discs

Disc Number	FDD Mixture Concentration (g of Krytox/ 100 ml Vertrel)	FTIR Absorbance at 1313 cm^{-1}	Average Krytox 16256N Thickness (Å)
191	1.0	0.0174, 0.0175, 0.0176	80
201	1.0	0.0155, 0.0155, 0.0163	70
216	1.0	0.0141, 0.0145, 0.0151	60
196	3.0	0.0460, 0.0483, 0.0485	230
208	3.0	0.0566, 0.0569, 0.0572	280
240	3.0	0.0538, 0.0541, 0.0549	270
188	5.0	0.0724, 0.0759, 0.0769	400
189	5.0	0.0751, 0.0761, 0.0766	400
244	5.0	0.0755, 0.0761, 0.0791	350

The data in Table 4 indicate the accumulated error associated with surface-to-surface reproducibility and lubricant uniformity across any one surface are within

± 15%. The three Krytox thickness ranges studied were 60-80, 230-280, and 350-400 Å, which correlate to FDD Krytox 16256N concentrations of 1.0, 3.0 and 5.0 g in 100 ml of Vertrel 245, respectively. Several wear tracks were worn on each 440C disc listed in Table 4 and the mean friction coefficient was recorded as a function of the number of disc rotational cycles for each one. A typical plot of mean friction coefficient vs. cycle number is shown in Figure 7. These particular datum were taken on the center wear track of disc #201 with a Krytox film ~70 Å thick and show the mean friction coefficient begins to rise from ≤ 0.3 near 200 cycles and crosses the failure line of 0.63 at ~370 cycles. Hence, in this case, the lubricant lifetime is 370 cycles. Each data point below the failure line exhibited a maximum variation about the mean friction coefficient over the rotational cycle that was 0.03, whereas this variation approached 0.05 near the failure line (friction coefficient > ~0.55). Beyond the point of failure, while the mean friction coefficient remained above the failure line of 0.63, variations over the rotational cycle grew to ~0.1. These larger variations were also considered an indicator of failure. Unless otherwise stated, other lubricated mean friction coefficient values will have similar deviations.

The plots of mean friction coefficient vs. cycle number of each wear track tested were all similar in appearance to that of Figure 7. Regardless of Krytox thickness, the initial mean friction coefficient of each wear track was approximately 0.3, thus verifying boundary lubrication. However, after performing a number of the tests it was apparent that the lifetimes had a significant spread in their values for each of the three general Krytox thicknesses. These spreads in lifetime appeared to be
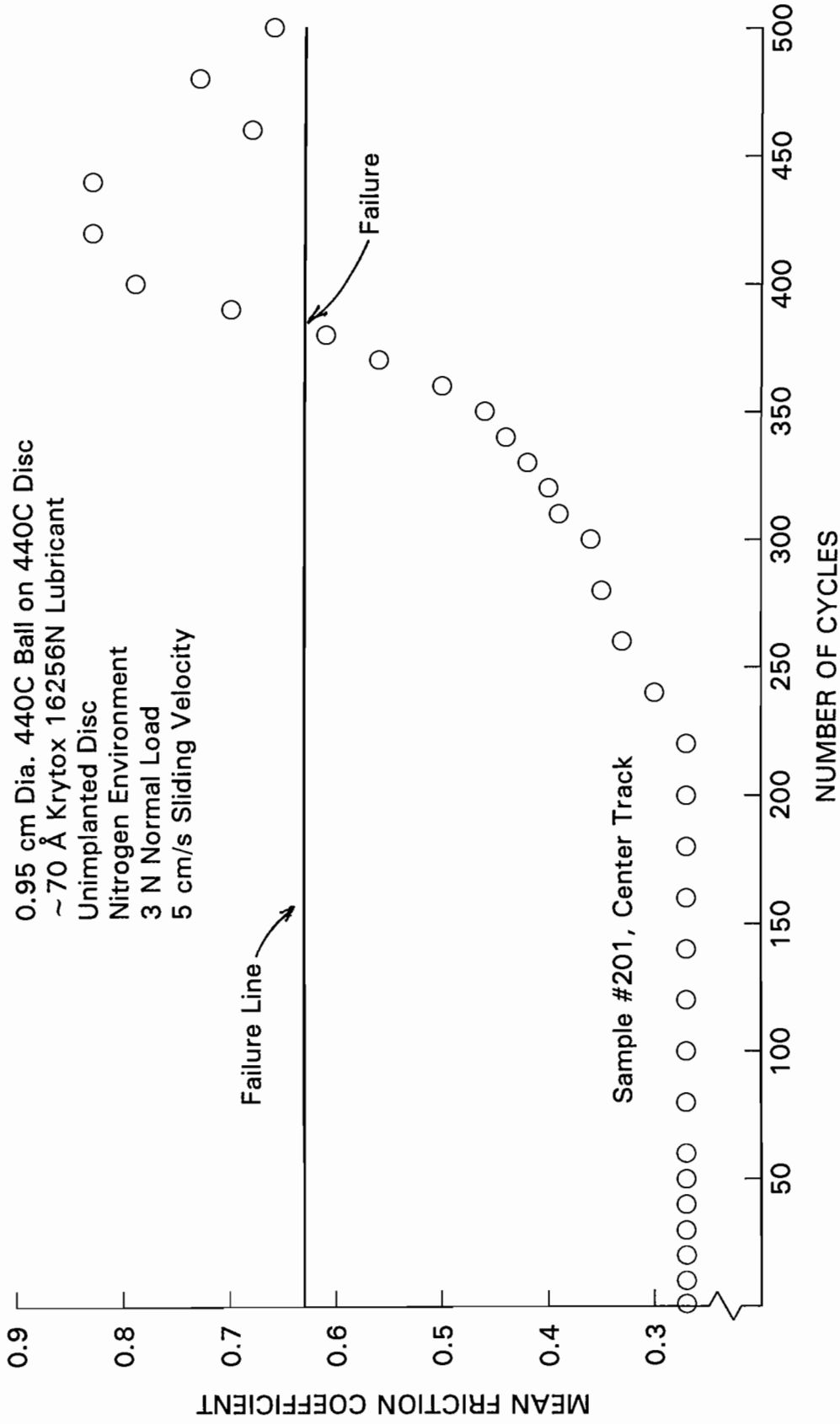
Figure 7. Typical Friction Coefficient Data for Unimplanted, Lubricated Discs

random, as they were not dependant upon either a particular sample or wear track (i.e. inner, middle or outer tracks).

When tests had been performed on all of the discs listed in Table 4, considerable scatter in the lifetimes associated with each specific film thickness was observed. In order to make these scattered results meaningful, it was decided that they should be presented using Weibull statistics.[67] Weibull statistics have been used since it was first introduced in 1951 in many applications involving data spread. The data obtained for the discs listed in Table 4 for the 60-80 Å lubricant thickness values are plotted in Fig. 8 using Weibull statistics. This plot shows the fraction of a group of samples that can be expected to fail (i.e. exceed 0.63 friction coefficient) as a function of the number of sliding contact cycles. The straight line drawn through the data represents the most probable failure history for the samples (i.e. the median-rank line). This line suggests 1% of a given number of tests can be expected to undergo failure at or before ~40 cycles and 10% should have failed at or before ~110 cycles.

The slope of the median-rank line describes the reproducibility of the data, with an infinite slope indicating all failures occur as the same number of cycles are completed (100% reproducibility). For the data of Fig. 8, the Weibull slope is 2.1. Given an infinite number of tests, the 90% confidence bands indicate the region that the lifetimes of 90% of them are predicted to fall. These bands are quite similar for each data set, so only the median-rank lines will be shown in subsequent plots.

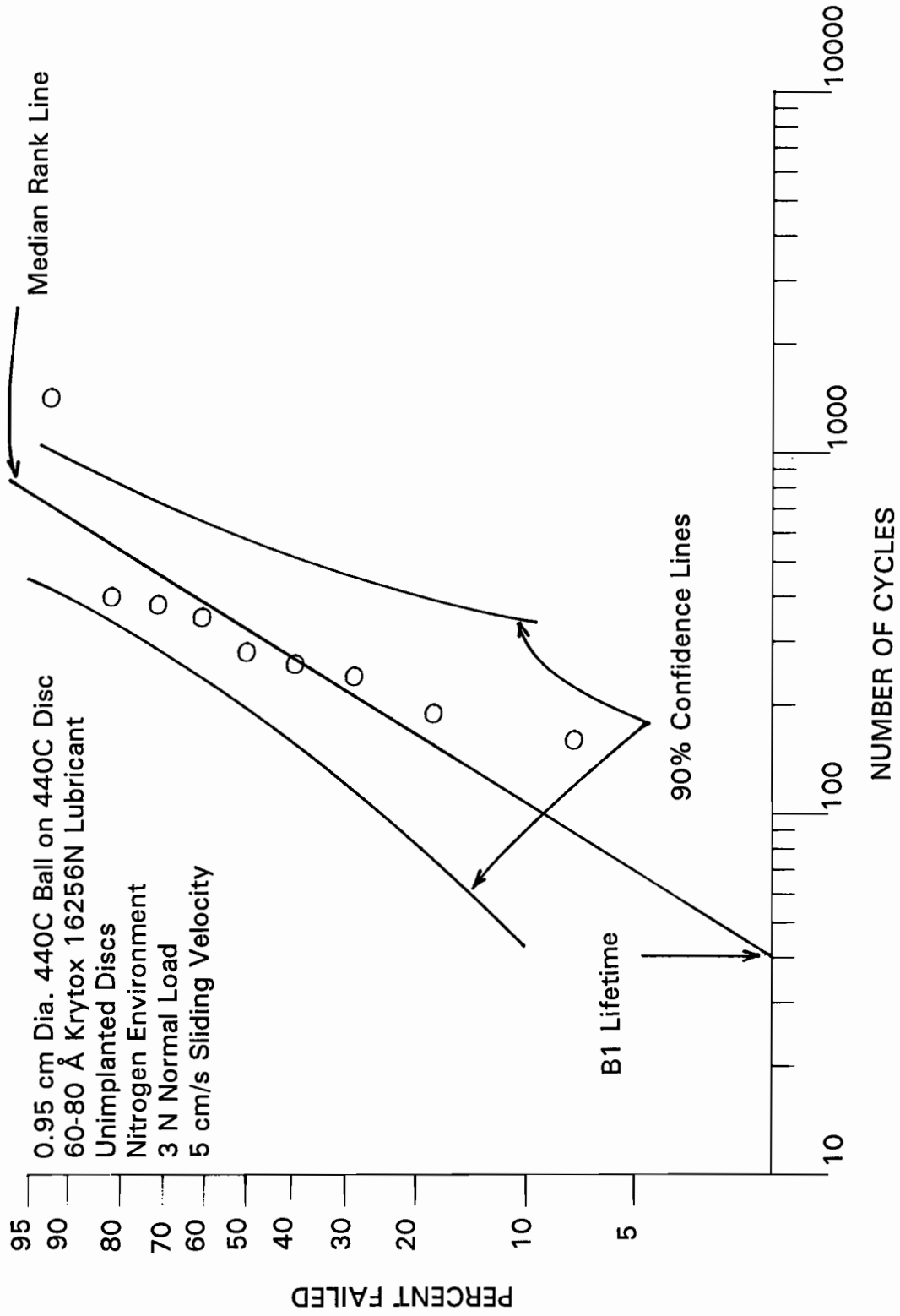The usefulness of a Weibull plot can be demonstrated by relating it to the

35

Figure 8. Weibull Distributions of Lifetimes for Unimplanted, Lubricated Discs

reliability of a component. For a typical space mechanism, which cannot generally be retrieved for maintenance, reliability is very important. If $>99\%$ reliability is desired in a lubricated couple, then the number of cycles that it is allowed to experience should be less than the value that will generally produce failure 1% of the time (frequently called the B1 lifetime). For the data of Fig. 8, it is about 40 cycles (the intersection of the median-rank line and the horizontal 1% failure line). Frequently, the characteristic life is also cited. It is the number of cycles at the 63.2% failure condition and it is ~380 cycles for these data.

Weibull data obtained for the three lubricant thickness ranges associated with the data of Table 4 (60-80, 230-280 and 350-400 Å) are shown in Figure 9. They are considered reasonable in that they show the shortest lifetimes for the thinnest film and generally the longest for the thickest one although lifetimes are about the same for the thickest and intermediate films. The fact that the thicker films have about the same median-rank lines suggests that excess lubricant that is pushed aside as the ball passes plays a role in these cases. This excess lubricant can re-enter the contact area immediately after ball passage, thereby replenishing the films and inducing longer lifetimes. This mechanism is also considered consistent with the somewhat greater lifetimes for the thickest coatings and the decrease in Weibull slope (2.1 to 1.6 to 1.2) that accompanies the increase in film thickness. The slope change is considered to be related to variability in lubricant flow for the very thin films being studied. Because tests conducted with discs coated with 60-80 Å Krytox films required less time to complete and also yielded the greatest Weibull slopes, this lubricant thickness was
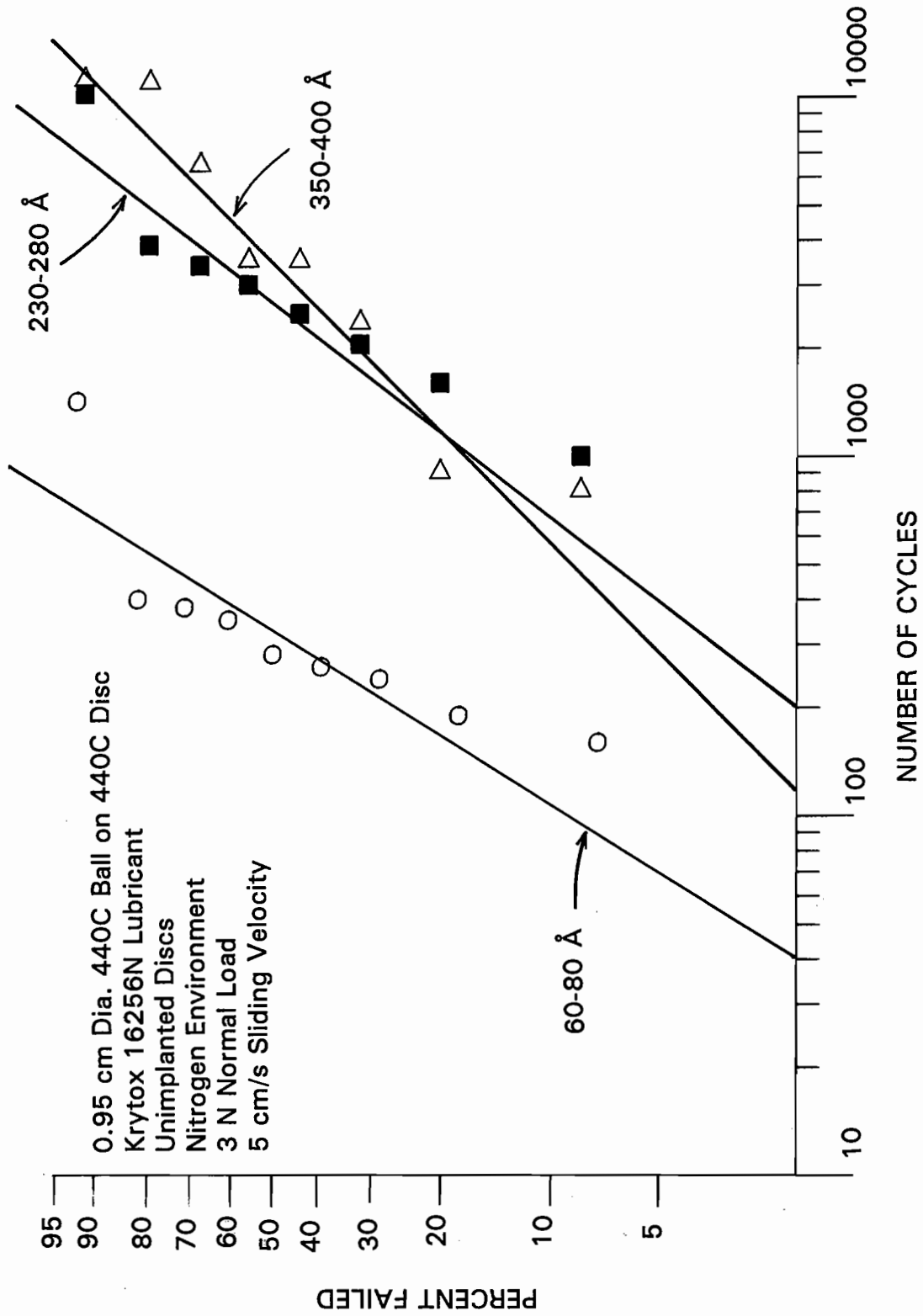
Figure 9. Effect of Lubricant Thickness on Weibull Distribution Lifetimes for Unimplanted 440C Discs

38

selected as the standard and was used for subsequent testing.

D. Implanted - Lubricated Disc Tests

Tribo-testing results obtained from implanted discs coated with a 60-80 Å thick layer of Krytox were compared to corresponding results obtained on unimplanted discs. The designations of the samples tested, along with FTIR absorbance peak height and mean Krytox thickness data for the implanted discs, are shown in Table 5. The FTIR data indicate the film thicknesses are uniform within $\pm$ 15% of the tabulated values.

Typical mean-friction-coefficient histories measured on one of the several tracks worn on each of the implanted discs identified in Table 5 are compared to the history of an unimplanted disc in Fig. 10. Figure 10a shows complete histories to failure for the discs and Fig. 10b is a blow-up showing more detail of their early failure-histories. The unimplanted-lubricated-disc data are reproduced from Figure 8 as the solid squares.

The friction coefficients for all of the discs are initially near 0.3 and for the cases shown, the shortest and longest lifetimes are ~ 10 cycles (carbon implanted) and ~ 3800 cycles (Titanium implanted), respectively, compared to ~ 380 cycles from the unimplanted one. The other three implantation conditions resulted in lubricated lifetimes between the two extremes (~ 80 cycles for titanium+nitrogen, ~ 220 cycles for nitrogen and ~ 1200 for titanium+carbon).

39

Table 5. FTIR Absorbance and Film Thickness Data for Implanted-Lubricated 440C Discs (FDD Concentration - 1.0 g of Krytox 16256N in 100 ml of Vertrel 245)

Surface Treatment (Disc Designation)	FTIR Absorbance at 1313 cm^{-1}	Average Krytox Thickness (Å)
Titanium Implanted No Backfill (165)	0.0196, 0.0204, 0.0204	80
(167)	0.0154, 0.0164, 0.0164	70
(179)	0.0150, 0.0180, 0.0200	80
Titanium Implanted N$_2$ Backfill (153)	0.0178, 0.0182, 0.0185	80
(171)	0.0176, 0.0178, 0.0185	80
Titanium Implanted CH$_4$ Backfill (174)	0.0174, 0.0191, 0.0197	80
(175)	0.0179, 0.0181, 0.0195	80
(177)	0.0191, 0.0200, 0.0202	80
N$_2$ Implanted (141)	0.0162, 0.0170, 0.0171	70
(169)	0.0140, 0.0142, 0.0146	60
(183)	0.0157, 0.0160, 0.0160	70
C Implanted (173)	0.0177, 0.0193, 0.0210	80
(181)	0.0152, 0.0158, 0.0168	70

The shapes of each of the friction-coefficient-history curves shown in Fig. 10 are typical of those observed for each of the several tests conducted on discs implanted at a prescribed condition. Lifetimes, however, generally fell over a sufficiently wide range for each condition so it was best to again consider the data using Weibull statistics. Weibull plots comparing the lubricant-failure characteristics of the five sets of implanted discs to the characteristics of the unimplanted discs are

Figure 10. Typical Friction History Showing Effect of Ion Implantation
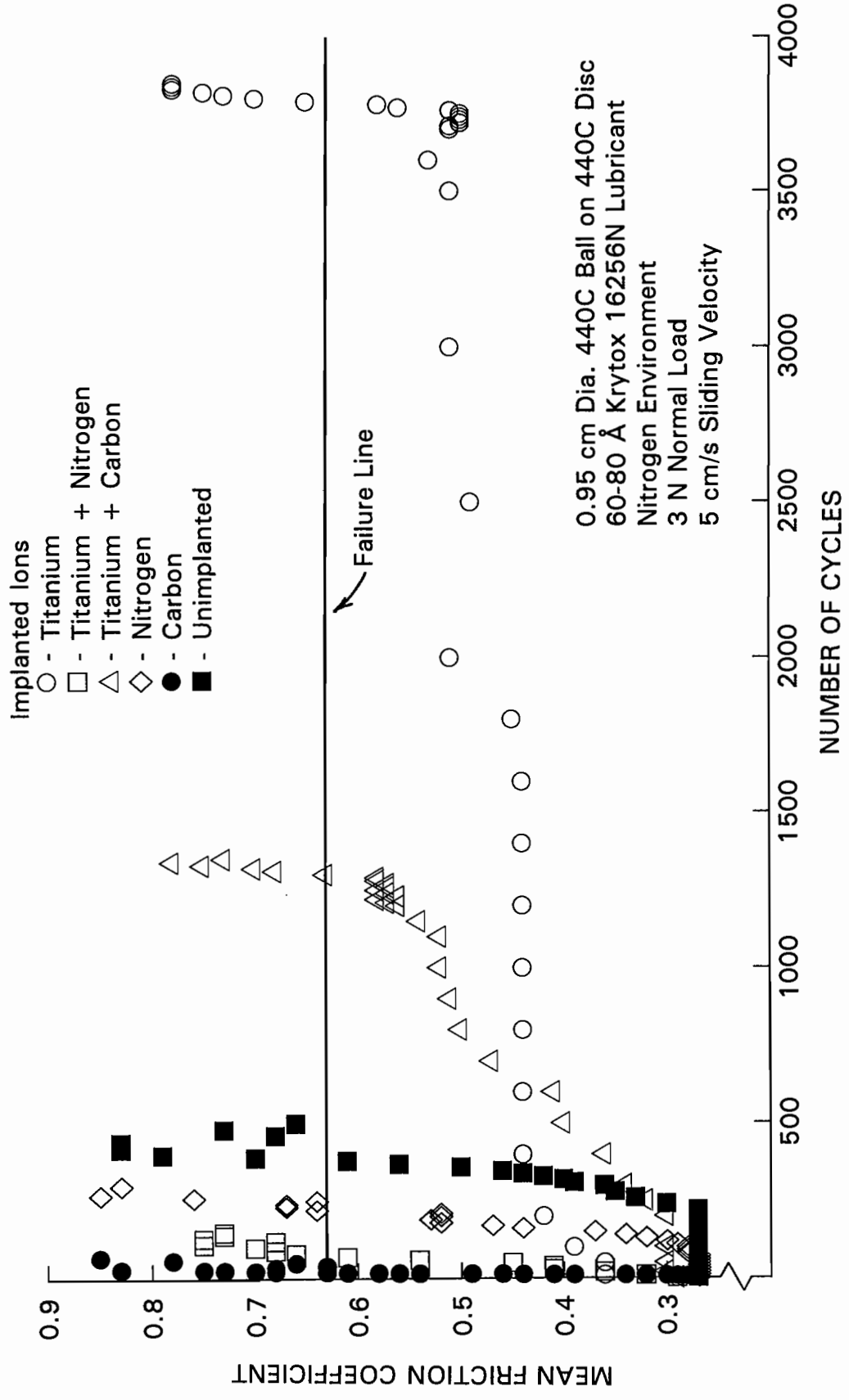
a. Complete History to Failure

Figure 10. Typical Friction History Showing Effect of Ion Implantation

shown in Figures 11 through 15, in the order of their appearance in Table 5. In each figure circles and solid squares symbolize the lubricant lifetime data for unimplanted and implanted discs, respectively. It is noted that each data point fell within the 90% confidence bands about the median rank line associated with the complete set for that condition. The data are, therefore, considered representative and consistent.

Figure 11 shows that titanium implantation of 440C discs induces almost an order of magnitude increase in the various lifetimes of the Krytox-lubricated surface. It also induces an increase in the Weibull slope from 2.1 for the unimplanted disc to 3.5 for the implanted one. The 99% reliability, or B1 life, for the titanium-implanted disc is ~950 cycles compared to ~40 cycles for the unimplanted one, a 24-fold improvement. The characteristic life of the disc was also increased from ~380 to ~3560 cycles by implanting it with Ti.

Figures 12 through 15 also yield lifetime and Weibull-slope data and are summarized in Table 6. These results show that titanium implantation with CH_4 backfill also improves the lubricant lifetime, but all other implanted species (titanium with nitrogen backfill, nitrogen implantation and carbon implantation) degrade the lifetimes. The low Weibull slope induced by titanium implantation with nitrogen backfill which is given in Table 6 is noteworthy. It suggests very poor reproducibility, yields a B1 lifetime that is less than unity and is probably unrealistic.
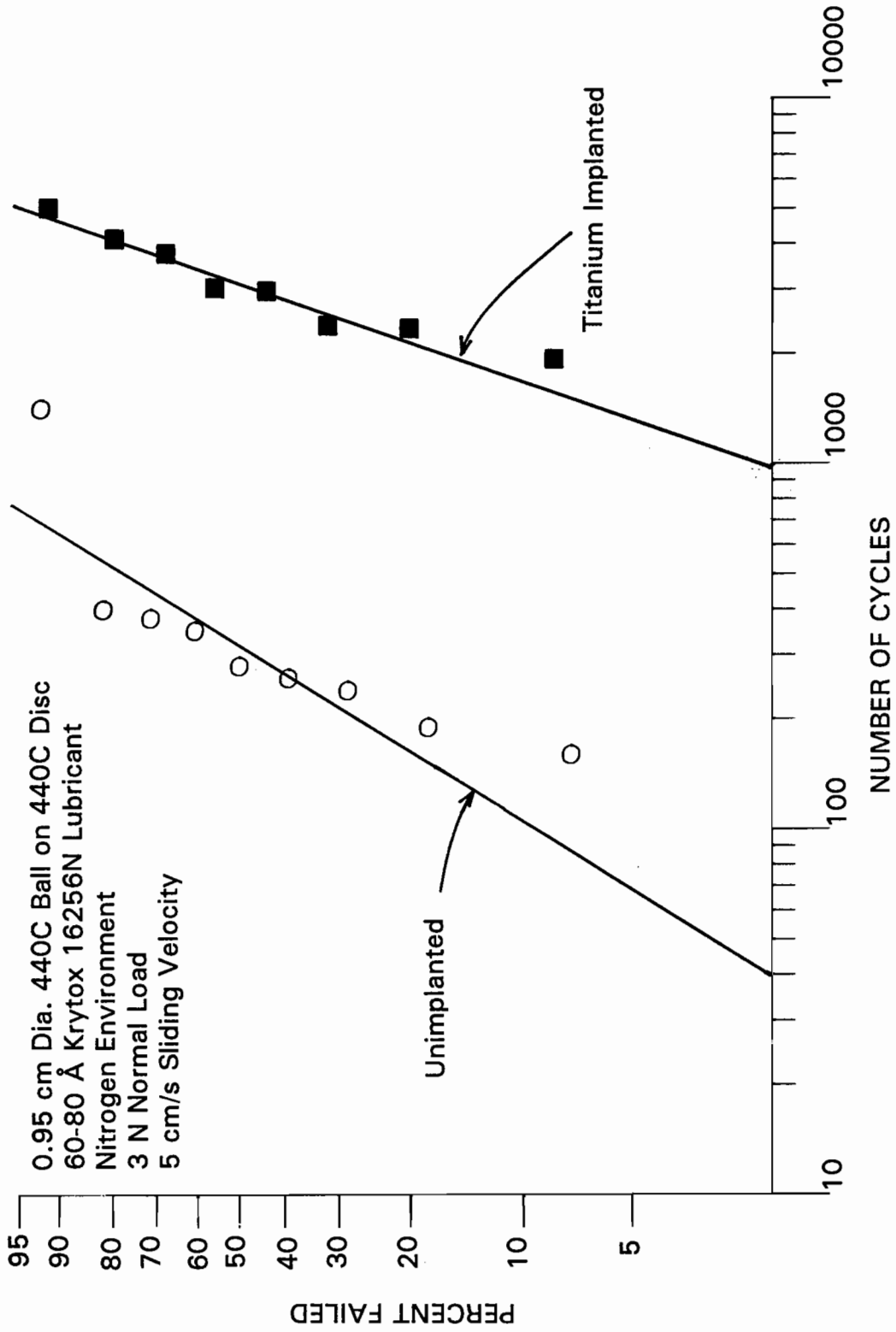
Figure 11. Effect of Titanium Ion Implantation

44
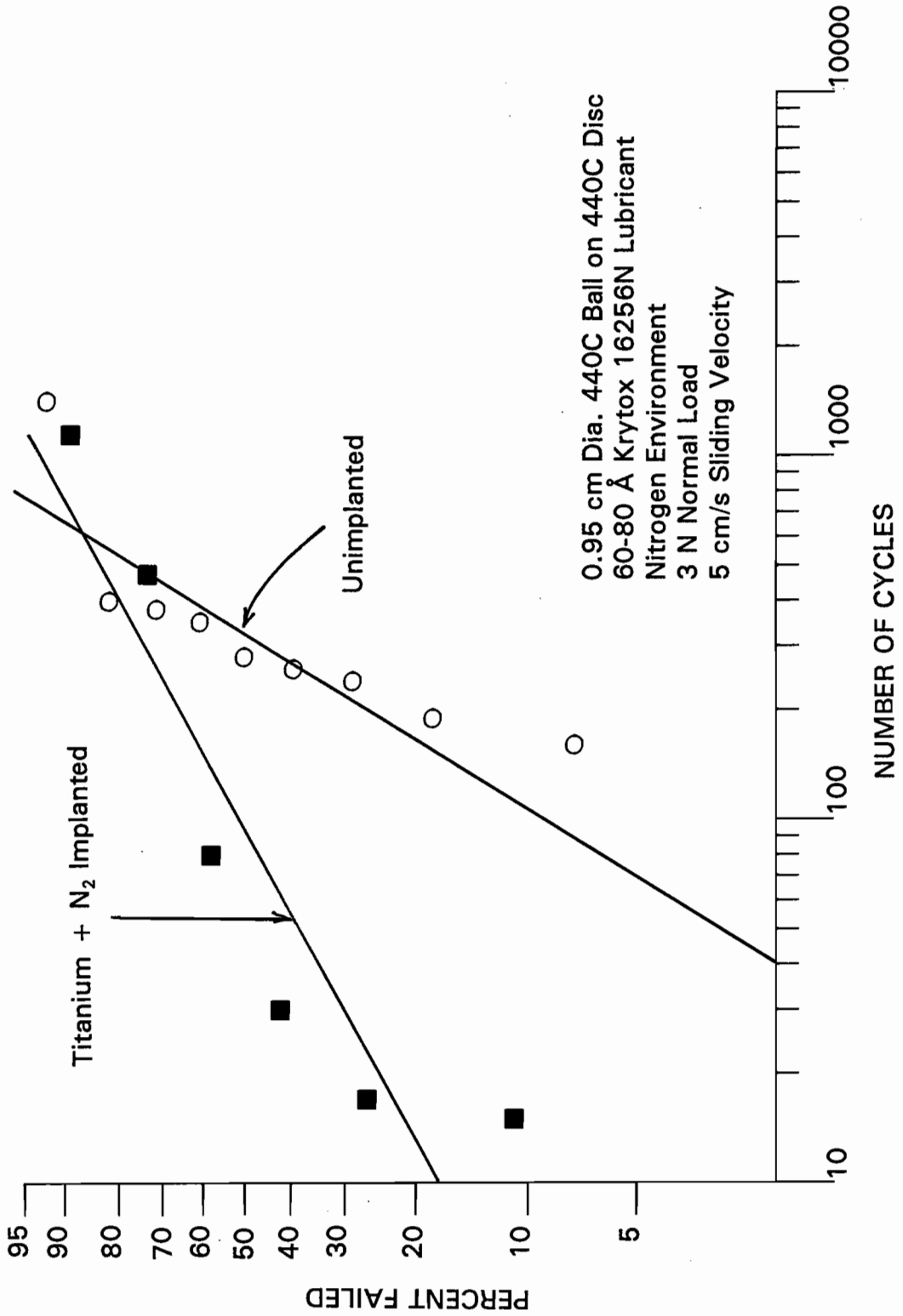
Figure 12. Effect of Titanium + N_2 Ion Implantation

0.95 cm Dia. 440C Ball on 440C Disc
60-80 Å Krytox 16256N Lubricant
Nitrogen Environment
3 N Normal Load
5 cm/s Sliding Velocity

Unimplanted

Titanium + N_2 Implanted

NUMBER OF CYCLES

PERCENT FAILED

45
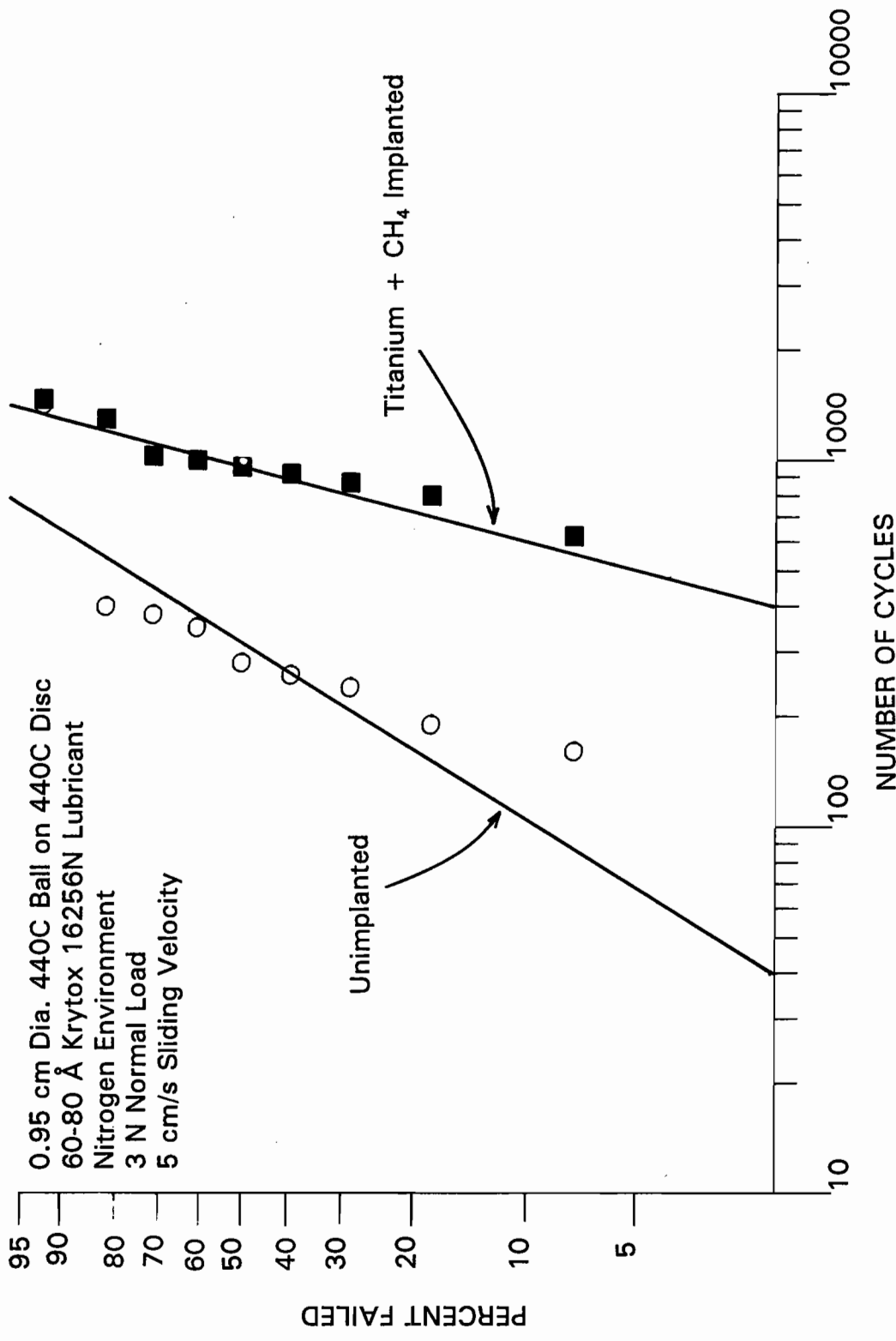
Figure 13. Effect of Titanium + CH$_4$ Ion Implantation
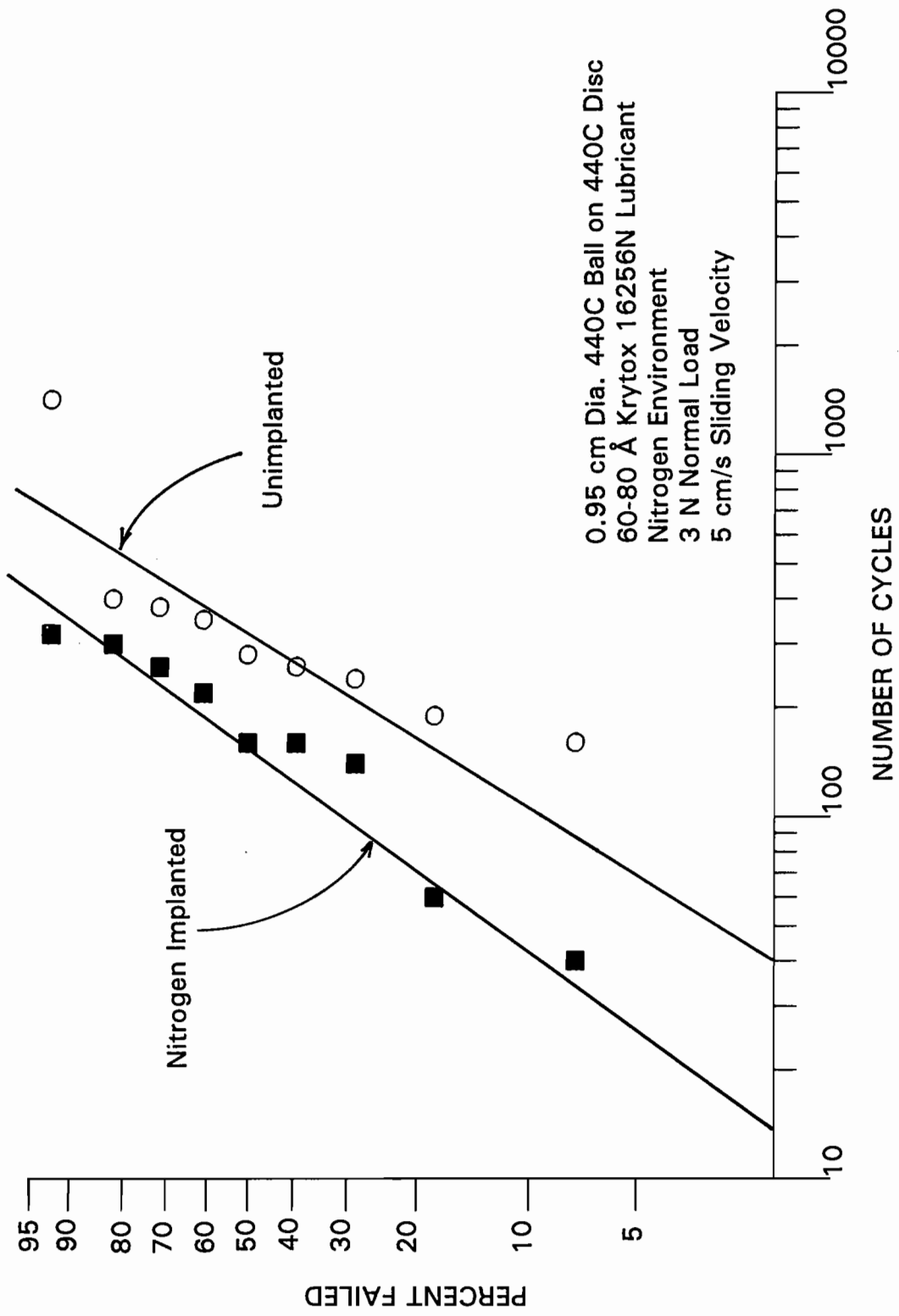
Figure 14. Effect of Nitrogen Ion Implantation

0.95 cm Dia. 440C Ball on 440C Disc
60-80 Å Krytox 16256N Lubricant
Nitrogen Environment
3 N Normal Load
5 cm/s Sliding Velocity

Unimplanted

Nitrogen Implanted

NUMBER OF CYCLES

PERCENT FAILED
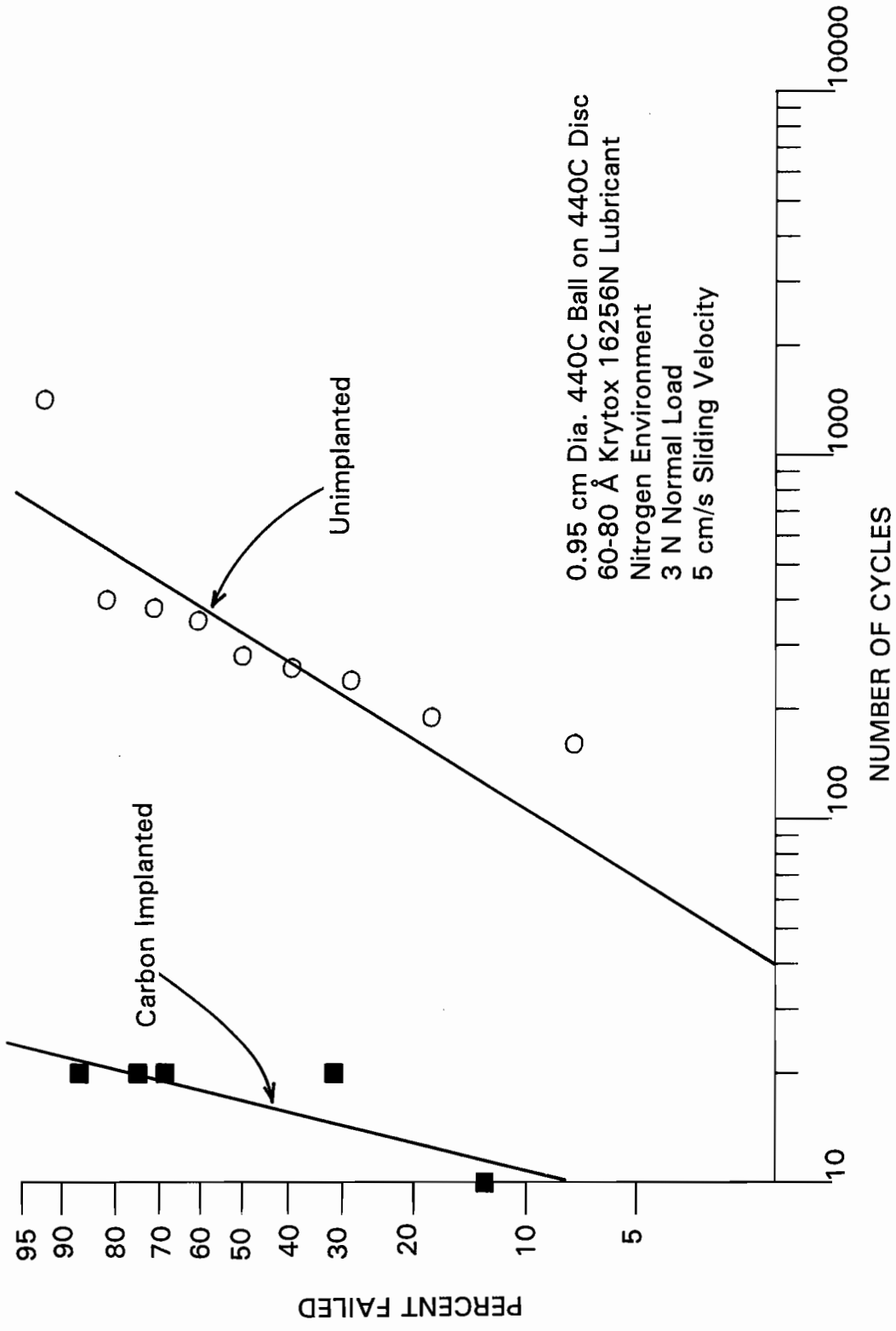
Figure 15. Effect of Carbon Ion Implantation

48

Table 6. Summary of Data Obtained from Weibull Plots

Surface Treatment	B1 Life (Cycles)	Characteristic Life (Cycles)	Weibull Slope
Unimplanted	40	380	2.1
Ti Implanted	950	3560	3.5
Ti Implanted N_2 Backfill	--	190	0.6
Ti Implanted CH_4 Backfill	400	1090	4.5
N_2 Implanted	10	210	1.6
CH_4 Implanted	< 10	20	4.2

E. Surface Microstructural and Compositional Data

It was anticipated that differences in disc microstructures and compositions induced by the implantation of the various ions might suggest a mechanism by which lubricant lifetimes were changed. Hence, X-ray diffraction (XRD) and conversion electron Mössbauer spectroscopic (CEMS) measurements were made on one disc from each implantation condition. Figure 16 shows XRD spectra measured on these discs. All of them show the strong peaks at ~43° and ~65° that are characteristic of a martensitic/ferritic phase. The peak at ~51° is due in part to an austenite phase, whose presence was confined by a resolved peak at ~75°. The other peaks are characteristic of a metal carbide phase ($M_{23}C_6$ where M = Fe or Cr).

There are some slight differences between the unimplanted and implanted-disc spectra that reflect changes induced by implantation. For example, the spectra of the
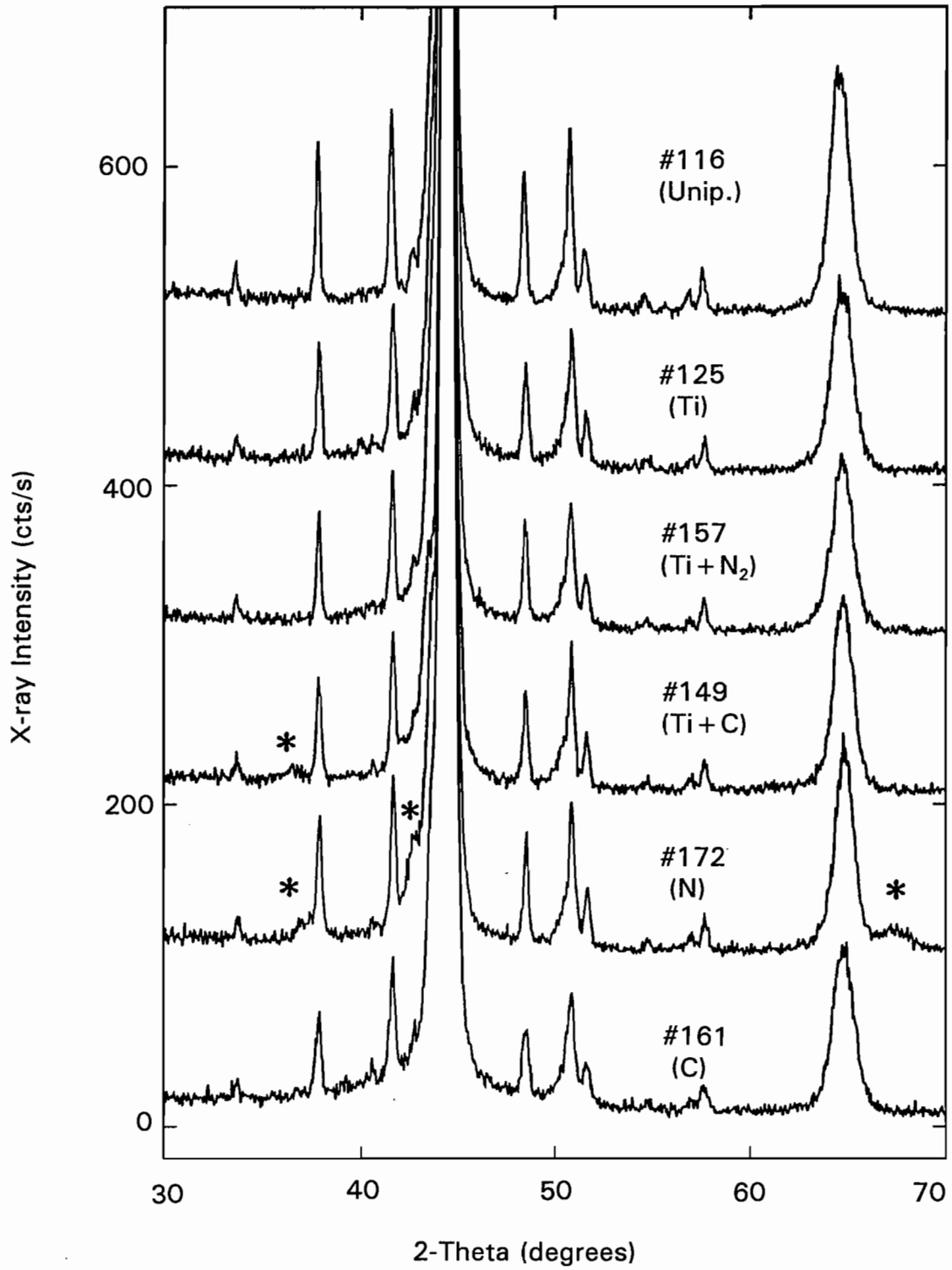
Figure 16. Typical X-Ray Diffraction Spectra for Unimplanted (Unip.) and Implanted Discs (Implanted Species)

titanium implanted (#125, Ti) and the titanium+nitrogen implanted (#157, Ti+N)

discs are identical to the spectrum for the unimplanted disc (#116, Unip.). This

suggests that the Ti and Ti+N implanted layers may either be too shallow to be

detected by XRD or amorphous. The slight peak marked by an asterisk on the

spectrum for the titanium+carbon implanted disc (#149, Ti+C) is indicative of TiC

and this suggests a shallow layer of TiC was formed on this disc. The peaks

identified by asterisks on the nitrogen-implanted-disc (#172, N) spectrum indicate an

ϵ-$(Fe,Cr)_{2+x}N$ phase formed on this disc.[35] Finally, it is observed that the XRD

spectrum of the carbon-implanted disc (#161, C) has a very broad, weak peak at

$\sim 43°$ suggesting an amorphous Fe-Cr-C phase may have formed on this disc.

Figure 17 shows Mössbauer (CEMS) spectra for the same discs represented by

the data of Fig. 16. They consist of measured data points; an overall, solid curve-fit

line through the data; and dotted lines representing subspectra of the microstructural

components that yield the overall curve fit. The microstructures that correspond to

each of the subspectra are indicated by stick diagrams beneath the various spectra.

For example, the stick diagrams under the trace for disc #116 correspond to a

magnetic martensite/ferrite phase (designated F) and austenite + metal carbide phases

(designated A + $M_{23}C_6$, where M = Cr mostly, and Fe).[71,73,74] These two distinct

phases produce signals that are not resolved.

Comparison of all of the spectra suggests that the 0.1-μm-thick surface layer

on all of the discs include a significant amount of the martensitic/ferrite and

austenitic/carbide phases. The titanium-implanted-disc surface layer contains, in
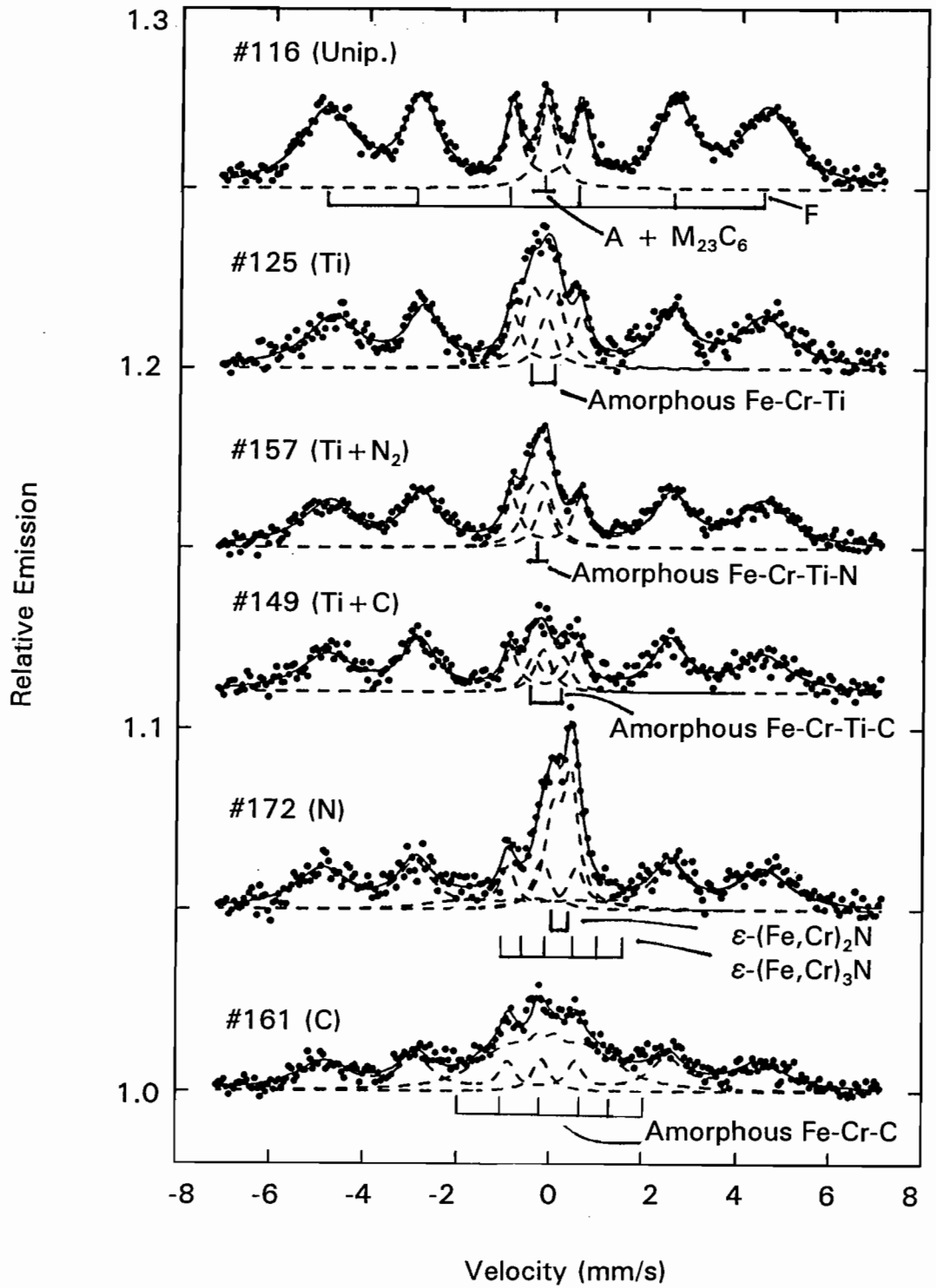
Figure 17. Typical Conversion Electron Mössbauer Spectra for Unimplanted (Unip.) and Implanted Discs (Implanted Species). Stick Figures Indicate Dominant Microstructures (A, F, ε, etc.)

addition, a significant amount of an amorphous Fe-Cr-Ti phase.[70-72] Surface layers

on the titanium+nitrogen, titanium+carbon and carbon implanted discs also contain

slightly different amorphous phases.[70-72] It is because these phases are amorphous that

no evidence of them can be seen in the XRD spectra of Fig. 16 (except possibly #161

as noted previously). The microstructural phases indicated in Fig. 17 are summarized

in Table 7. It is noteworthy that the TiC observed in the XRD spectrum for the

titanium+carbon implanted disc cannot be detected by CEMS because CEMS is

sensitive to Fe-containing compounds only. It is probably because some Ti is

consumed to form the TiC in this disc that the amount of amorphous phase in it is

less than in the Ti and Ti+N implanted discs (as indicated by the lower amorphous-

signal intensity for the Ti+C implanted disc). Finally, CEMS detected the presence

of a hexagonal ε-$(Fe,Cr)_{2+x}N$ like phase in the nitrogen implanted disc.[35,38,73]

If one accepts the postulates that 1) longer lubricant lifetimes are realized

when the formation of the Lewis acid FeF_3 is inhibited and 2) Lewis acid formation is

inhibited via a passivating surface microstructure produced through ion implantation,

then it is reasonable to correlate surface microstructures and lifetimes. Such a

correlation based on the results of this study suggest the microstructures ranked from

most to least effective are: amorphous Fe-Cr-Ti > amorphous Fe-Cr-Ti-C + TiC >

unimplanted 440C $\geq$ ϵ-$(Fe,Cr)_xN$ [x = 2 or 3] > amorphous Fe-Cr-Ti-N $\simeq$

amorphous Fe-Cr-C.

Table 7. Summary of the XRD and CEMS Results.

Surface Treatment (Disc Designation)	Phase
Unimplanted (#116)	F = martensite/ferrite A + $M_{23}C_6$ = austenite/metal carbide mixture
Titanium Implanted No backfill (#125)	F A + $M_{23}C_6$ amorphous Fe-Cr-Ti
Titanium Implanted N_2 Backfill (#157)	F A + $M_{23}C_6$ amorphous Fe-Cr-Ti-N
Titanium Implanted CH_4 Backfill (#149)	F A + $M_{23}C_6$ amorphous Fe-Cr-Ti-C TiC*
N_2 Implanted (#172)	F A + $M_{23}C_6$ ϵ-(Fe,Cr)$_2$N ϵ-(Fe,Cr)$_3$N
C Implanted (#161)	F A + $M_{23}C_6$ amorphous Fe-Cr-C

* This phase was detected with XRD but cannot be detected with CEMS.

IV. DISCUSSION

The data of Figs. 11-15 and Table 6 show quite clearly that the lifetime of Krytox 16256N on a 440C disc sliding against a 440C ball can be altered significantly by implanting a thin layer on the disc with various ions. The reason for these changes is uncertain, but it is known that implantation can induce both chemical and microstructural changes in materials. It is also known that PFPE oils can degrade as a result of chemical reaction with a surface and that the rate of the degradation is a strong function of temperature. In addition, it could be that implantation alters the way in which the PFPE molecules attach to the disc and that this, in turn, changes the shear stress they experience and, therefore, the likelihood that they will be torn apart mechanically. Hence it is suggested that ion implantation could alter the lifetime of a PFPE film by changing the rate of 1) mechanical scission of the molecular chains and/or 2) chemical degradation in the thermal environment of tribo-contact. The following discussion addresses the likelihood that these mechanisms are significant.

A. Mechanical Scission

It has been observed that the shear stress at a boundary lubricated tribological contact can result in the fracture of lubricant bonds (mechanical scission).[75] In the

present case, the maximum value of this shear stress can be estimated by dividing the frictional force by the Hertzian contact area between the pin and disc. Since the applied normal load (3 N) is the same for all tests and the implanted layers are so thin they should not affect the contact area significantly, one expects the shear stress to be directly proportional to the friction coefficient. Hence, initially, when the friction coefficient is near 0.3 for all lubricated discs, the common Hertzian contact area and shear stress are calculated to be 6.5×10^{-9} m^2 and 140 MPa, respectively, for all of the tests. This information cannot be used to determine whether lubricant bonds will be broken, however, without additional information like the number of molecular layers and their orientation in the lubricant film.

Because friction coefficient determines the shear stress and these coefficients varied over the same ranges and showed no dramatic changes at a friction coefficient below the failure value, it is argued that mechanical scission was the same for all of the discs. This, in turn, suggests that mechanical scission was probably not a significant contributor to differences in tribological lifetime induced by ion implantation.

B. Chemical Degradation

It has been established that a PFPE-lubricated, 440C couple in boundary contact will eventually result in the formation of the Lewis acid FeF$_3$.[7,9,10,14-16] It has been inferred that this same reaction 1) will occur and will probably be accelerated under tribological conditions and 2) will lead to the degradation of the tribo-properties

56

of the PFPE lubricant. It has also been argued that the more readily the Lewis acids

form and the stronger they are, the quicker the PFPE will degrade. A passivation

layer that inhibits Lewis acid formation would, therefore, be expected to increase the

effective lifetime of the lubricant.

The rate of Lewis acid formation is determined by the temperature in the

440C/PFPE reaction zone and the appropriate temperature is uncertain. It could

range from the bulk surface/lubricant temperature to peak values reached as asperities

on the two sliding surfaces contact and heat is released. This uncertainty is reflected

in the literature. For example, Carrè attributes the degradation of PFPE lubricant in

sliding/rolling contact to high asperity temperatures.[9,13] However, Mori and Morales[16]

and Herrera-Fierro et al.[7] suggest asperity temperatures are not relevant.

In order to model asperity temperature properly, one must consider heat

dissipation into the disc, bearing ball and lubricant. Such a model is beyond the

scope of this work, but a model of dry (unlubricated) contact, which can be used to

estimate the upper limit on asperity temperatures, has been developed by Ashby et

al.[76,77] This model has been used to obtain the asperity and bulk-surface temperature

data plotted as dotted and solid lines, respectively, as a function of normal load (F)

and relative sliding velocity in Fig. 18. These results reflect the geometry (ball on

flat), thermal and mechanical material properties (440C steel couple), and radius of

the area of contact between the ball and disc (R_o). The quantity A_n, which appears in

the Hertzian pressure (the argument of the ordinate), is the nominal contact area

(πR_o^2). Hertzian stress calculations indicate the value of R_o is 0.04 mm at the
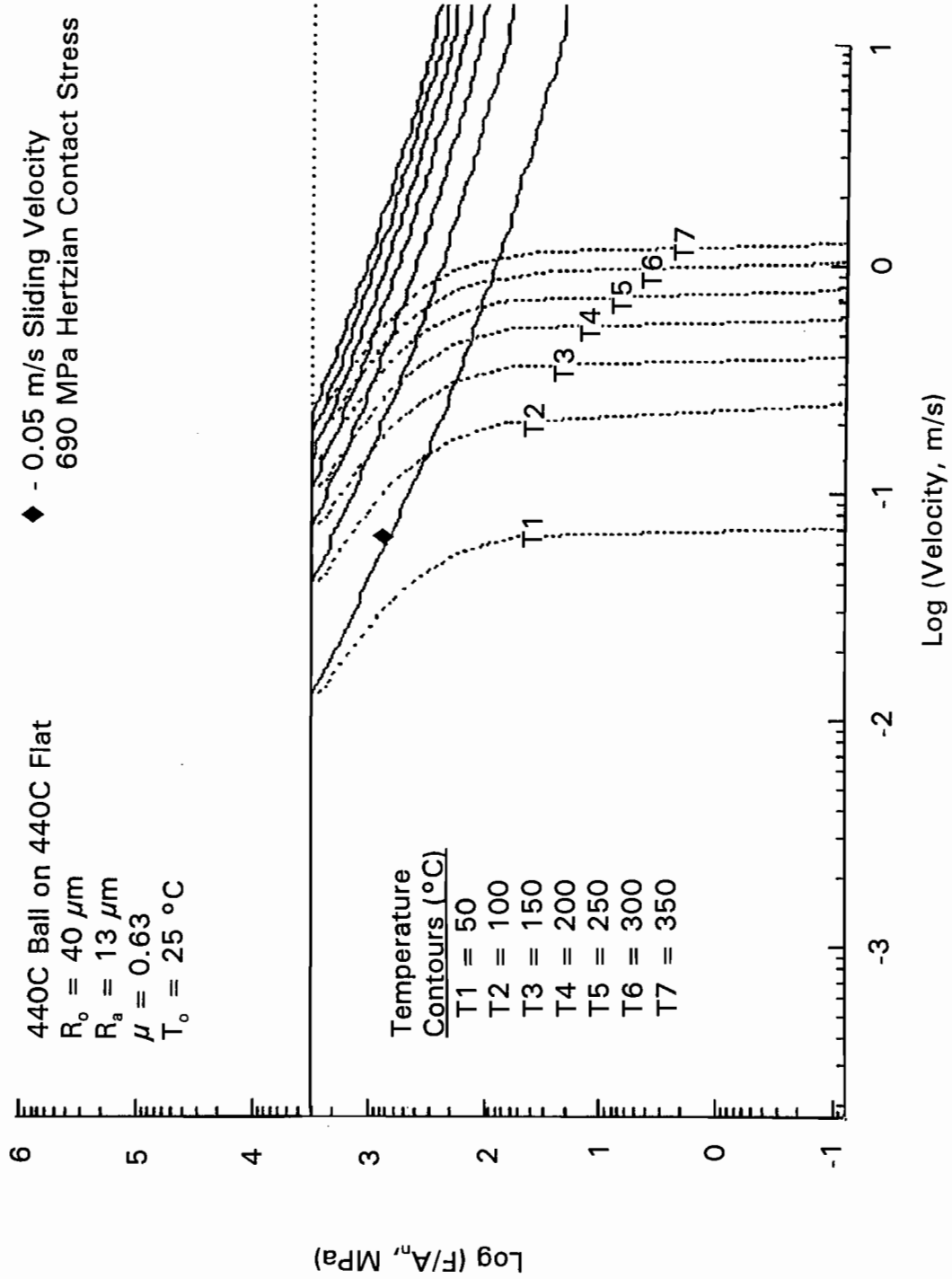
57

Figure 18. Temperature Map for an Unlubricated 440C Ball on 440C Disc in Sliding Contact.

3 N normal load used so the contact area is 5×10^{-9} m^2 and the Hertzian pressure is 690 MPa. Other inputs required in the model to obtain the results in Fig. 18 were the friction coefficient, ambient temperature and the asperity radius. The values used were 1) the failure value of friction coefficient (0.63), 2) a 25° C ambient temperature and 3) an asperity radius (13×10^{-6} m) obtained from an expression given by Ashby.[77] This expression ($R_a = 0.1/H$) requires the hardness (H) of 440C steel (7500 MPa) as an input. At the initial test condition (a contact stress of 690 MPa and a sliding velocity of 0.05 m/s as identified by the solid diamond) the data of Fig. 18 indicate the bulk temperature will be ∼50 °C and the asperity temperature will be ∼70 °C.

Since implantation generally hardens a surface,[35,38,41,54] and the asperity radius decreases with hardness, it is logical to expect implantation to cause asperity temperatures to increase. However, the Ashby-model shows that reducing the asperity radius to 6.7 μm (half of the Fig. 18 value and corresponding to doubling the hardness) induced only a 15% increase in the bulk and asperity temperatures. Even these temperature, which are conservatively high because the effects of lubricant are neglected, are well below the 200-300°C needed to induce rapid breakdown of PFPE on 440C steel.[7] Hence, these results suggest that temperatures in the reaction zone are not elevated sufficiently to induce rapid reaction rates.

V. CONCLUSIONS

An ultra-thin film of Krytox lubricant (60-400 Å) can be applied to flat metal discs inexpensively, reproducibly and uniformly ($\pm15\%$) using a film deposition device. Characteristic lifetimes of these boundary-lubricant films can be determined by measuring the number of pin-on-disc, sliding-wear cycles required to induce an increase in the friction coefficient from an initial value characteristic of the lubricated wear couple to a final or failure value characteristic of the unlubricated, unimplanted couple. A sufficient number of tests must be conducted to assure that results analyzed using Weibull statistics will be meaningful.

Ion implantation of 440C steel discs with Ti, Ti+N, Ti+C, N or C all cause the number of unlubricated sliding-wear-cycles-to-failure to increase from near zero for the unimplanted 440C couple to about 10 cycles. The characteristic lifetimes of 60-80 Å thick perfluoropolyether (Krytox 16256N) films on 440C steel discs worn against 440C balls can be altered significantly by ion implanting the disc before the lubricant film is applied. The B63.2 (characteristic life) and B1 lifetimes of the 440C couple were increased by an order of magnitude and a factor of 24, respectively, by implanting with Ti. Implantation with Ti+C also induced improvements in these lifetimes, but implantation with Ti+N, N and C did not. Ranked from most to least effective, the implanted species were:

$$Ti > Ti + CH_4 > unimplanted > N_2 > C \simeq Ti + N_2.$$

The mechanism postulated to explain changes in lubricant lifetime induced by ion implantation involves the formation of passivating or reacting layers that inhibit or facilitate the production of a Lewis acid that breaks down the Krytox lubricant. The surface microstructures produced by the implantation ranked from most to least effective in enhancing lubricant lifetime are:

amorphous Fe-Cr-Ti > amorphous Fe-Cr-Ti-C + TiC > unimplanted 440C > ϵ-(Fe,Cr)$_x$N, x = 2 or 3 > amorphous Fe-Cr-C $\simeq$ amorphous Fe-Cr-Ti-N.
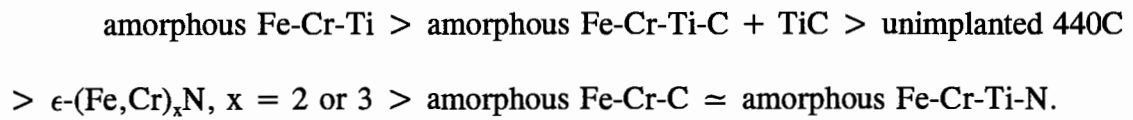
VI. REFERENCES

1. Jones, W.R., Jr.: "The Properties of Perfluoropolyethers Used for Space Applications," NASA TM-106275, July 1993.

2. Fusaro, R.L., and Khonsari, M.M.: "Liquid Lubrication for Space Applications," NASA TM-105198, July 1992.

3. Fleischauer, P.D., and Hilton, M.R.: "Assessment of the Tribological Requirements of Advanced Spacecraft Mechanisms," Aerospace Report No. TOR-0090(5064)-1, 1991.

4. Rowntree, R.A., and Todd, M.J.: "A Review of European Trends in Space Tribology and Its Application to Spacecraft Mechanism Design," Mat. Res. Soc.Symp. Proc., V. 140, 1989, pp. 21-34.

5. Watson, N.D., Miller, J.B., Taylor, L.V., Lovell, J.B., Cox, L.W., Fedors, J.C., Kopia, L.P., Holloway, R.M., and Bradley, O.H.: "Earth Radiation Budget Experiment (ERBE) Scanner Instrument Anomaly Investigation," NASA TM-87636, Oct. 1985.

6. Jones, W.R., Jr., Private Communications, May-Oct. 1993, NASA Lewis Research Center, Cleveland, Ohio.

7. Herrera-Fierro, P., Jones, W.R., Jr., and Pepper, S.V.: "Interfacial Chemistry of a Perfluoropolyether Lubricant Studied by X-ray Photoelectron Spectroscopy and Temperature Desorption Spectroscopy," J. Vac. Sci. Technol. A, V. 2, N. 11, Mar/Apr 1993.

8. Herrera-Fierro, P., Pepper, S.V., and Jones, W.R., Jr.: "An XPS Study of the Stability of Fomblin Z25 on the Native Oxide of Aluminum," NASA TM-105594, Prepared for the 38th National Symposium of the American Vacuum Society, Seattle, WA, Nov 1991.

9. Carré, D.J.: "Perfluoropolyalkylether Oil Degradation: Inference of FeF_3 Formation on Steel Surfaces Under Boundary Conditions," ASLE Trans., V. 29, N. 2, 1986, pp. 121-125.

10. Carré, D.J.: "The Performance of Perfluoropolyalkylether Oils Under Boundary Lubrication Conditions," ASLE Trans., V. 31, N. 4, 1987, pp. 437-441.

11. Hayashida, K., Yamamoto, K., and Nishimura, M.: "Wear and Degradation Characteristics of Perfluoroalkylpolyethers (PFPEs) in High Vacuum," STLE Preprint No. 93-AM-1B-1, Presented at the 48th Annual Meeting in Calgary, Alberta, Canada, May 1993.

12. Carré, D.J., Fleischauer, P.D., Kalogeras, C.G., and Marten, H.D.: "Comparison of Lubricant Performance in an Oscillating Spacecraft Mechanism," Trans. of the ASME, V. 113, April 1991, pp. 308-312.

13. Carré, D.J.: "The Use of Solid Ceramic and Ceramic Hard-Coated Components to Prolong the Performance of Perfluoropolyalkylether Lubricants," SSD-TR-9032, Sept. 1990.

14. Carré, D.J.: "The Performance of Perfluoropolyalkyethers Under Boundary Conditions," SSD-TR-91-17, April 1991.

15. Mori, S., and Morales, W.: "Decomposition of Perfluoroalkylpolyethers (PFPE) in Ultra-High Vacuum Under Sliding Conditions," Tribology Transactions, V. 33, N. 3, 1990, pp. 325-332.

16. Mori, S., and Morales, W.: "Tribological Reactions of Perfluoroalkylpolyether Oils with Stainless Steel Under Ultrahigh Vacuum Conditions at Room Temperature," Wear, V. 132, 1989, pp. 111-121.

17. Stevens, K.T.: "Some Observations on the Performance of Fomblin Z25 Oil and Braycote-3L-38RP Grease in Ball Bearings and Gear Boxes," ESA SP-196, Dec. 1983.

18. Novotny, V.J., Karis, T.E., and Johnson, N.W.: "Lubricant Removal, Degradation, and Recovery on Particulate Magnetic Recording Media," Journal of Tribology, V. 114, Jan. 1992, pp. 61-67.

19. Baxter, B.H., and Hall, B.P.: "The Use of Perfluoroether Lubricants in Unprotected Space Environments," Proc. 19th Aerospace Mech. Symp., NASA CP-2371, 1985.

20. Kasai, P.H.: "Perfluoropolyethers: Intramolecular Disproportionation," Macromolecules, V. 25, 1992, pp. 6791-6799.

21. Kasai, P.H., and Wheeler, P.: "Degradation of Perfluoropolyethers Catalyzed by Aluminum Chloride," Applied Surface Science, V. 52, 1991, pp. 91-106.

22. Kasai, P.H., Tang, W.T., and Wheeler, P.: "Degradation of Perfluoropolyethers Catalyzed by Aluminum Oxide," Applied Surface Science, V. 51, 1991, pp. 201-211.

23. Helmick, L.A., and Jones, W.R., Jr.: "Determination of the Thermal Stability of Perfluoropolyalkyl Ethers by Tensimetry," NASA TM-106081, Prepared for the Society of Tribologists and Lubrication Engineers Annual Meeting sponsored by the Society of Tribologists and Lubrication Engineers, Philadelphia, Pennsylvania, May 1992.

24. Carré, D.J., and Markowitz, J.A.: "The Reaction of Perfluoropolyalkylether Oil with FeF_3, AlF_3, and $AlCl_3$ at Elevated Temperatures," ASLE Trans., V. 28, N. 1, 1985, pp. 40-46.

25. Jones, W.R., Jr., Paciorek, K.J.L., Ito, T.I., and Kratzer, R.H.: "Thermal Oxidative Degradation Reactions of Linear Perfluoroalkyl Ethers," R. H. Ind. Eng. Chem. Prod. Res. Dev., V. 22, June 1983, pp. 166-170.

26. Jones, W.R., Jr., Paciorek, K.J.L., Harris, D.H., Smythe, M.E., Nakahara, J.H., and Kratzer, R.H.: "The Effects of Metals and Inhibitors on Thermal Oxidative Degradation Reactions of Unbranched Perfluoroalkyl Ethers," R. H. Ind. Eng. Chem. Prod. Res. Dev., V. 24, Sept. 1985, pp. 417-420.

27. Paciorek, K.J.L., Kratzer, R.H., Kaufman, J., and Nakahara, J.H.: "Thermal Oxidative Studies of Poly(hexafluoropropene Oxide) Fluids," Journal of Applied Polymer Science, V. 24, 1979, pp. 1397-1411.

28. Sharma, S.K., Gschwender, L.J., and Snyder, C.E., Jr.: "Development of a Soluble Lubricity Additive for Perfluoropolyalkylether Fluids," Journal of Synthetic Lubrication, V. 7, N. 1, 1990, pp. 15-23.

29. Srinivasan, P., Corti, C., Montagna, L., and Savelli,P.: "Soluble Additives for Perfluorinated Lubricants," JSL, V. 10, N. 2, 1993, pp. 143-164.

30. Basset, D., and Hermant, M.: "Oil-Soluble Fluorinated Compounds as Antiwear and Antifriction Additives," ASLE Transactions, Preprint No. 83-LC-2B-2, 1983.

31. Baker, M.A., Holland, L., and Laurenson, L.: "The Use of Perfluoralkyl Polyether Fluids in Vacuum Pumps," Vacuum, V. 21, N. 10, 1972, pp. 479- 481.

32. Loomis, W.R., and Fusaro, R.L.: "Liquid Lubricants for Advanced Aircraft Engines," NASA TM-104531, Aug. 1992.

33. Krytox® Vacuum Products and Services, Dupont, 1987.

34. Hartley, N.E.W., Swindlehurst, W.E., Dearnaley, G., and Turner, J.F.: "Friction Changes in Ion-Implanted Steel," Journal of Materials Science, V. 8, 1973, pp. 900-904.

35. Wei, R., Wilbur, P.J., Sampath, W.S., Williamson, D.L., and Wang, L.: "Sliding Wear of Nitrogen Ion-Implanted Stainless Steels," Lubrication Engineering, V. 47, N. 4, Apr. 1991, pp. 326-334.

36. Williamson, D.L., Wei, R., and Wilbur, P.J.: "Effects of Rapid, High-Dose, Elevated Temperature Ion Implantation on the Microstructure and Tribology of Ferrous Surfaces," Nuclear Instruments and Methods in Physics Research, V. 57, B56, 1991, pp. 625-629.

37. Williamson, D.L., Wang, L., Wei, R., and Wilbur, P.J.: "Solid Solution Strengthening of Stainless Steel Surface Layers by Rapid, High-Dose, Elevated Temperature Nitrogen Ion Implantation," Materials Letters, V. 9, N. 9, May 1990, pp. 302-308.

38. Wei, R., Wilbur, P.J., Sampath, W.S., Williamson, D.L., and Wang, L.: "Effects of Ion Implantation Conditions on the Tribology of Ferrous Surfaces," Journal of Tribology, V. 113, Jan. 1991, pp. 166-173.

39. Wei, R., Wilbur, P.J., Ozturk, O., and Williamson, D.L.: "Tribological Studies of Ultrahigh Dose Nitrogen-Implanted Iron and Stainless Steel," Nuclear Instruments and Methods in Physics Research, V. 60, B59, 1991 pp. 731-736.

40. Wei, R., Wilbur, P.J., Sampath, W.S., Williamson, D.L., Qu, Y., and Wang, L.: "Tribological Studies of Ion-Implanted Steel Constituents Using an Oscillating Pin-on-Disk Wear Tester," Journal of Tribology, V. 112, Jan. 1990, pp. 27-36.

41. Wei, R., Shogrin, B., Wilbur, P.J., Ozturk, O., Williamson, D.L., Ivanov, I., and Metin, E.: "The Effects of Low-Energy-Nitrogen-Ion-Implantation on the Tribological and Microstructural Characteristics of AISI 304 Stainless Steel," to be published.

42.   Singer, I.L., Bolster, R.N., Sprague, J.A., Kim, K. Ramalingam, S., Jeffries, R.A., and Ramseyer, G.O.: "Durable Metal Carbide Layers on Steels Formed by Ion Implantation at High Temperatures," <u>Journal of Applied Physics</u>, V. 58, N. 3, Aug. 1985, pp.1255-1258.

43.   Pope, L.E., Yost, F.G., Follstaedt, D.M., Picraux, S.T. and Knapp, J.A.: "Friction and Wear Reduction of 440C Stainless Steel By Ion Implantation," <u>Mat. Res. Soc. Symp. Proc.</u>, V. 27, 1984, pp.661-666.

44.   Singer, I.L., and Jeffries, R.A.: "Effects of Implantation Energy and Carbon Concentration on the Friction and Wear of Titanium-Implanted Steel," <u>Applied Physics Letters</u>, V. 43, N. 10, Nov. 1983, pp. 925-927.

45.   Singer, I.L., and Jeffries, R.A.: "Surface Chemistry and Friction Behavior of Ti-Implanted 52100 Steel," <u>Journal of Vacuum Science and Tech. A</u>, V. 1, N. 2, Apr-June 1983, pp.317-321.

46.   Fayeulle, S., and Singer, I.L.: "Friction Behavior and Debris Formation of Titanium-Implanted 52100 Steel," <u>Materials Science and Engineering</u>, A115, 1989, pp. 285-290.

47.   Misra, M.S., and Kustus, F.M., Edited by Clayton, C.R., and Preece, C.M.: "Corrosion Resistance of Ion Implanted 303 Stainless Steel, 52100 Bearing Steel, and 2024-T3 Aluminum Alloy," <u>Corrosion of Metals Processed by Directed Energy Beams</u>, 1981.

48.   Chabica, M.E., Williamson, D.L., Wei, R., and Wilbur, P.J.: "Microstructure and Corrosion of Nitrogen Implanted AISI 304 Stainless Steel," <u>Surface and Coatings Technology</u>, V. 51, 1992, pp. 24-29.

49.   Lo Russo, S., Mazzoldi, P., Scotoni, I., Tosello, C., and Tosto, S.: "Fatigue-Life Improvement by Nitrogen-Ion Implantation on Steel: Dose Dependence," <u>Applied Physics Letters</u>, V. 10, N. 36, May 1980, pp. 822-823.

50.   Wilbur, P.J., and Wei, R.: "High Current-Density Metal-Ion Implantation," <u>Rev. Sci. Instrum.</u>, V. 63, N. 4, April 1992, pp. 2491-2493.

51.   Wilbur, P.J., and Daniels, L.O.: "The Development and Application of an Ion Implanter Based on Ion Thruster Technology," <u>Vacuum</u>, V. 36, 1986, pp. 5-9.

52.   Sampath, W.S., Wei, R., and Wilbur, P.J.: "Ultrahigh Current Density Ion Implantation," <u>Journal of Metals</u>, V. 39, 1987, pp. 17-19.

53.   Singer, I.L., and Jeffries, R.A.: "Processing Steels for Tribological Applications by Titanium Implantation," <u>ASLE Transactions</u>, V. 28, N. 1, 1984, pp. 134-138.

54.   Wei, R.: "Tribological Studies of Ion-Implanted Steel Constituents," Colorado State University Ph.D. Dissertation, Mechanical Engineering Department, 1990.

55.   Lauer, J.L., and Jones, W.R., Jr.: "Friction Polymers," ASLE Special Publications SP-21, Tribology and Mechanics of Magnetic Storage Systems, Vol. III, pp. 14-23, Oct. 1986.

56.   Vig, J.R.: "UV/Ozone Cleaning of Surfaces," SLCET-TR-86-6, May 1986.

57.   Sowell, R.R., Cuthrell, R.E., Mattox, D.M., and Bland, R.D.: "Surface Cleaning by Ultraviolet Radiation," <u>J. Vac. Sci. Technol.</u>, V. 11, N. 1, Jan./Feb. 1974, pp. 474-475.

58.   Poulis, J.A., Cool, J.C., and Logtenberg, E.H.P.: "UV/Ozone Cleaning, a Convenient Alternative for High Quality Bonding Preparation," Int. J. <u>Adhesion and Adhesives</u>, V. 13, N. 2, April 1993, pp. 89-96.

59.   Jayne, D.J., Private Communication, May-Aug. 1993, NASA Lewis Research Center, Cleveland, Ohio.

60.   Scarati, A.M., and Caporiccio, G.: "Frictional Behaviour and Wear Resistance of Rigid Disks Lubricated with Neutral and Functional Perfluoropolyethers," <u>IEEE Transactions on Magnetics</u>, V. Mag.-23, N. 1, Jan. 1987, pp. 106-108.

61.   Brame, E.G., Jr. and Grasselli, J. (Editors): "Infrared and Raman Spectroscopy, Part A," <u>Practical Spectroscopy Series</u>, V. 1, 1976.

62.   Nakamoto, K.: <u>Infrared and Raman Spectra of Inorganic and Coordination Compounds</u>, Fourth Edition, 1986.

63.   Pepper, S.V., Private Communications, May-August 1993, NASA Lewis Research Center, Cleveland, Ohio.

64.   Pepper, S.V.: "Characterization and Application of a Grazing Angle Objective for Quantitative Infrared Reflection Microspectroscopy," to be published.

65. Shigley, J.E., and Mitchell, L.D.: "Hertz Contact Stresses," <u>Mechanical Engineering Design</u>, 4th Edition, 1983, pp. 85-87.

66. Ludema, K.C., Private Communications, July 1994, Engineering Conference, Ann Arbor, Michigan.

67. Johnson, L.G.: <u>The Statistical Treatment of Fatigue Experiments</u>, Elsevier Publishing Company, Inc., 1964.

68. Cohen, R.L.: "Elements of Mössbauer Spectroscopy," <u>Applications of Mössbauer Spectroscopy</u>, V. 1, 1976, pp. 1-33.

69. Greenwood, N.N. and Gibb, T.C.: "The Mössbauer Effect," <u>Mössbauer Spectroscopy</u>, 1971, pp. 1-29.

70. Williamson, D.L., Singer, I.L., Wei, R., and Wilbur, P.J.: "Amorphous Fe-Ti-C Phase Produced by Ion Implantation of Iron and Its Role in Tribological Behavior," <u>Nuclear Instruments and Methods in Physics Research</u>, B76, 1993, pp.210-212.

71. Williamson, D.L., Kustas, F.M., Fobare, D.F., and Misra, M.S.: "Mössbauer Study of Ti-Implanted 52100 Steel," <u>J. Appl. Phys.</u>, V. 60, N. 4, 1986, pp. 1493-1500.

72. Williamson, D.L., Kustas, F.M., Qu, Yi, and Smith, S.R.: "Titanium and Carbon Implantation of Iron," <u>Hyperfine Interactions</u>, V. 42, 1988, pp. 1029-1032.

73. Kustas, F.M., Misra, M.S., and Williamson, D.L.: "Microstructural Characterization of Nitrogen Implanted 440C Steel," <u>Nuclear Instruments and Methods in Physics Research</u>, B31, 1988, pp. 393-401.

74. Vardavoulias, M. and Papadimitriou, G.: Mössbauer Spectra and Hyperfine Parameters of Iron-Chromium Carbides in Ferritic Stainless Steel," <u>Phys. Stat. Sol.</u>, V. 134, 1992, pp.183-191.

75. Karis, T.E., Novotny, V.J., and Johnson, R.D.: "Mechanical Scission of Perfluoropolyethers," <u>Journal of Applied Polymer Science</u>, V. 50, 1993, pp. 1357-1368.

76. Ashby, M.F., Abulawi, J., and Kong, H.S.: "Temperature Maps for Frictional Heating in Dry Sliding," <u>Tribology Transactions</u>, V. 34, N. 4, 1991, pp. 577-587.

77.   Ashby, M.F., Kong, H.S., and Abulawi, J.: "Operation Manual for T-Maps, A Program for Constructing Maps for Surface Heating in Unlubricated Sliding," Version 2.0, June 1990.